PREDICTIVE DIGITAL MAPPING OF SOILS IN KITIMAT, BRITISH COLUMBIA

A Thesis Submitted to the Committee of Graduate Studies in Partial Fulfilment of the Requirements for the Degree of Master of Science in the Faculty of Arts and Science

TRENT UNIVERSITY

Peterborough, Ontario, Canada

Environmental and Life Sciences M.Sc. Graduate Program

December 2019

ABSTRACT

PREDICTIVE DIGITAL MAPPING OF SOILS IN KITIMAT, BRITISH COLUMBIA

Emily Olmstead

Soil is an essential natural resource that supports provisioning services such as agriculture, silviculture, and mining. However, there is limited knowledge on forest soil properties across Canada. Digital soil mapping may be used to fill these data gaps, as it can predict soil properties in areas with limited observations. The focus of this study was to develop predictive maps of select soil physicochemical properties for the Kitimat Valley, British Columbia, and apply these maps to assess the potential impacts of sulphur dioxide emissions from an aluminum smelter, on soil properties in the Valley. Exchangeable [Ex.] magnesium, organic matter, pH, coarse fragment, Ex. potassium, bulk density, Ex. calcium, Ex. acidity, and Ex. sodium were all mapped with acceptable confidence. Time to depletion of base cation pools showed that ~240 km2 of the study area had a depletion time of 50 years or less. However, sources of base cations such as atmospheric deposition and mineral weathering were not considered.

Keywords: Digital soil mapping, predictive mapping, regression kriging, soil properties, acidification, buffering capacity, sulphur deposition.

ACKNOWLEDGEMENTS

I would first like to thank supervisor, Julian Aherne for his continued guidance and understanding throughout this entire process. As well, I would like to thank my other committee members, Shaun Watmough and Tom Hutchinson for their guidance and encouragement.

There are quite a few colleagues who have helped me with my research who I would like to thank. Firstly, Phaedra Cowden, Patrick Levasseur, and Conor Gaffney, who were also sampling in the Kitimat Valley during the summer helped me complete my fieldwork in a timely fashion. Secondly. Kevin Adkinson, Grant Stott, and Matthew Moot also helped me in completing my lab analysis. Lastly, I would like to thank Holly Reid and Hazel Cathcart for their continued support in any and all matters related to R programming and QGIS.

This thesis was completed through graduate funding provided by an NSERC graduate research scholarship and an Ontario Graduate Scholarship awarded from Trent University. Without this funding, none of this research would have been possible, and I am forever grateful for the everything I have experienced through this program.

TABLE OF CONTENTS

LIST OF FIGURES

LIST OF TABLES

1.0 CHAPTER 1: GENERAL INTRODUCTION

1.1 FACTORS OF SOIL FORMATION

Soil is an essential resource; it provides ecosystem regulation (water filtration and nutrient storage for plant productivity) and underpins important ecosystem services such as provisioning (i.e., agriculture, silviculture, and precious metals). These provisions are key to the economic success and the support of growing populations in many countries. As such, it is important to effectively manage these natural resources; to do this, we need to understand the spatial variation of their chemical and physical properties.

Soils are comprised of varying mixtures of fragmented partially or completely weathered rocks, organic matter, water, air and living organisms. As soils develop, they form distinct layers which are called horizons; these horizons are created under specific soil forming conditions; the cross section of these horizons, or the soil profile, is used to identify soil types (Byers et al., 1938). There are many factors that influence the formation of soil, such as climate and topography, but it is important that the processes which turn geological materials such as rock, sand, and clay into parent material are identified. The first process these materials encounter is physical weathering; temperature changes occur and the expansion and contraction within the rock causes tension which causes weak areas to break and crumble. Additionally, in cool-temperate regions, water, which has filled the cracks in rock during the warmer months then freezes during the cold, causing further expansion and cracking. Plants have also been shown to cause expansion, as their roots fill crevasses and wedge rocks apart (Byers et al., 1938). Secondly, rock is turned into parent material through chemical weathering. Carbon dioxide (CO_2), which is found in the soil as a byproduct of organic matter breakdown or plant respiration, and water react in the soil to

form carbonic acid (H_2CO_3) (Andrews and Schlesinger, 2001). This H_2CO_3, along with other organic acids produced via microbial activity (oxalate, acetate, and citrate acids) stimulate mineral dissolution in soil and the release of base cations (Byers et al., 1938; Fox and Comerford, 1990; Jones, 1998; Oh and Richter, 2004). After the parent material of a region is developed from rock, the process of soil formation can begin (Jenny, 1941).

In 1883, Dokuchaev first discussed the idea that soil was a function of parent material, climate, vegetation, the age of the terrain and the topography. Then, in 1941, Jenny formalized a conceptual model to describe soil formation based on five main factors; this model was expressed as:

$$S = f(cl, o, r, p, t \ldots)$$

Where S is a measurable soil property, and f meaning "is a factor of", and clorpt represented the factors of soil formation: climate (cl), organisms (o), relief (topography; r), parent material (p), and time(t). Jenny made a distinction that these were considered factors because they were independent variables as opposed to causes or forces of soil formation. It was found that when this model was approached as a mathematical equation, it was not easily parameterized (Kline, 1973; Phillips, 1998, Stephens, 1947). Therefore, it was determined that it was instead to be used a conceptual model to show that soil formation occurs when variation is seen in one factor while the others remain relatively constant. This model has become one of the most popular concepts in pedology for understanding soil formation (Richards and Edmonds, 1987; Phillips, 1998).

Climate as a soil forming factor is broken down into two main variables, moisture and temperature. Moisture was identified as an important factor because as water percolates through the soil, soluble materials such as potassium and sodium are leached out and

carried to rivers and lakes via deep seepage. It was found that in areas of humid conditions, water is not readily held by soil particles, and so available materials are leached from the soil (Hilgard, 1914). It has also been found that in North America, areas of higher rainfall have higher clay content in the soil, due to increased weathering caused by the water movement through the soil (Coffey, 1912). Additionally, water has been shown to affect the size of soil aggregates, or particles, as it has been seen that aggregate size increased as rainfall increases (Baver, 1934). Temperature is important because it can dictate the rate of reactions which occur in the soil, such as chemical weathering; at temperatures below 0°C, chemical processes are practically stopped (van't Hoff, 1884). If weathering in the soil does not take place, soil formation is slowed, and no base cations are released, which is not conducive to vegetation productivity. As well, temperature determines the depth of weathering and soil formed; in colder climates like Canada, soil depths rarely exceed a meter, where tropical climates have much deeper soil profiles (Jenny, 1941). Lastly, temperature can determine the rate at which litter fall decomposes and is incorporated into the soil as organic matter; climates with warmer temperatures have seen much faster decomposition than colder climates (Waksman and Gerretsen, 1931).

Organisms (specifically microorganisms such as bacteria, and vegetation) have a role in soil formation; bacteria are often found on exposed rock faces, and they are also abundantly found in phases of rock decay, indicating they play a role in rock decomposition to form soils. As well, nitrogen fixing bacteria such as *Azobacter* are often found in soils and may influence the amount of nitrogen found in the soil (Blochlinger, 1931). Lastly, soil bacteria produce CO_2 in the process of breaking down soil organic matter, which can produce organic acids (Schlesinger, 1977). Vegetation can influence soil in many ways, as

roots hold soil particles together and prevent erosion, allowing for the formation of a soil profile (Braun-Blanquet and Jenny, 1926). As well, plant roots exploit fresh cracks exposed in rocks and continue to create spaces, breaking up larger rocks (Phillips et al., 2008). Roots have also been found to give off CO_2 as part of the respiration process, which as mentioned above has been found to increase the solubility of carbonates and continue the weathering and soil formation process (Andrews and Schlesinger, 2001; Oh and Ritcher, 2004). Vegetation has also been found to influence vertical water movement through the soil, as the development of roots creates space for water percolation, and water uptake by vegetation increases the upward movement of water (Wu et al., 1999). Lastly, vegetation may influence the amount of organic matter present in a soil, as litterfall and grasses are decomposed and incorporated into the humus layer of soil (Jenny, 1941)

Relief, or topography was deemed a factor of soil formation for two reasons; the first was the effect of relief on water movement. Ellis (1938) found that soils in areas of depression receive more water because they receive the same amount of rainfall as other areas, plus the runoff from the areas that surround it. Additionally, areas which are undulating or hilly, receive less water due to the same runoff processes. As discussed above, the amount of water which is percolated into the soil will determine leaching of nutrients and weathering depth of the soil. Relief has also shown to influence soil based on erosion; areas with steeper slopes and little vegetation (such as mountainous areas) are eroded through rainfall and wind processes, and much of the materials are transported from the higher elevations to the bottom of the slope, causing less developed soil profiles in the higher elevation areas and more developed soils in the lower elevations (Marbut, 1935).

Parent material, as was defined by Jenny (1941): the initial state of the soil system, or the geological material which soil has formed. There are many different types of bedrock material, with two main sub-groups being primary (residual) or secondary (transported) parent materials. Residual parent material occurs when bedrock such as igneous, sedimentary, or metamorphic rock is weathered in its original place, while transported parent material is comprised of materials which are deposited during glaciation (Byers et al., 1938). The parent material can influence soil formation as the different materials lend to the development of different soil properties once the parent material is weathered. For example, parent materials developed on igneous rock were found to have lower calcium, but higher potassium, and phosphorous than a parent material developed from calcareous bedrock (Leiningen 1912). As well, parent materials dictate texture (sand silt, and clay) as parent materials high in silicon and aluminum give way to produce clay, while quartz produces sandy soils. Soil texture in turn influences aggregation and water infiltration, which can influence leaching and deep soil weathering (Byers et al., 1938).

Time was the last soil formation factor identified by Jenny (1941). Most obviously, all the physical and chemical processes which occur in soil formation occur over time. It is seen that areas which were not glaciated have much deeper and more developed soil profiles than areas like north America, which have comparatively new soils. Depending on the other soil formation factors, these soils which have developed longer may be higher in organic matter, clays, and base cations, which may also contribute to a higher buffering capacity.

1.2 SOIL PHYSICOCHEMICAL PROPERTIES

There are many physical and chemical properties of soil that can be used to determine its quality. Soil quality is a concept that is based on the objectives of whoever is assessing it; for instance, in the case of forestry or agriculture, soil quality many be evaluated as the soils capacity for continued crop growth, or the support of biomass production (Shoenholtz et al., 2000). For this study, soil quality was defined more broadly, as was stated by Carter and MacEwan (1996), soil quality describes a soil condition that supports a healthy ecosystem.

Some well-known physical soil properties that are measured to determine soil quality are bulk density (Db), soil particle size (sand, silt, and clay), and coarse fragment (CF). Chemical soil properties used to assess soil quality are organic matter (OM), exchangeable cations, soil nutrient availability of nitrogen, phosphorous, and potassium (NPK) as well as pH. Bulk density is the proportion of soil and pore space in a given soil sample; it is used to evaluate soil compaction and influences root growth and water and oxygen supply (Larson and Pierce, 1991; Doran and Parkin, 1994). Organic matter is the proportion of soil which is comprised of various stages of decaying litter and detritus and represents a considerable carbon and nutrient reservoir in the soil (Lutzow and Koegel-Knabner, 2009). Soil particle size is the percentage of sand, silt, and clay that is present in a soil sample and influences many other soil processes such as water, oxygen and nutrient movement through the depths of the soil profile. For example, soils which have a higher sand content will have increased water flow but also less water retention, where soils containing more clay will have decreased water movement but higher water retention (Doran and Parkin, 1994). Lastly, CF is the proportion of soil which is greater than 2 mm.

In terms of chemical soil properties used to assess soil quality, OM is used to assess soil quality because it influences many other soil properties, such as: the aggregation of soil particles, and soil porosity (which then influences water and air movement). As well, it contains a considerable pool of carbon and nutrients such as nitrogen, phosphorous, and exchangeable cations (Henderson, 1995). Next, exchangeable cations, which are positively charged ions which are adsorbed to negatively charged exchange sites found on the soil exchange complex found as part of organic matter or clays in soils. The four major basic cations are calcium (Ca^{2+}), magnesium (Mg^{2+}), potassium (K^{+}), and sodium (Na^{+}), and the main acidic cations are aluminum (Al^{3+}) and H^{+} (Sumner and Miller, 1996; Sonon et al., 2014). These cations, depending on the acidity of the soil solution can "exchange" or be displaced from the exchange site in order to buffer other positively charged acidic ions such as H^{+} (Sonon et al., 2014; Tamminen and Starr, 1990). The major net sources of cations are chemical weathering of soil parent material and wet and dry atmospheric deposition; they are also cycled through vegetation as they are taken up as essential nutrients and released again as vegetation dies and decomposes (Ouimet and Duchesne, 2005; Schoenholtz et al., 2000). Soil nutrient availability is often assessed by soil concentrations of NPK, especially in the context of agriculture (Romig et al., 1996). These nutrients are often used to assess a soils capacity for plant (or crop) production (Reganold and Palmer, 1995; Aune and Lal, 1997). Lastly, Soil pH is important because as pH decreases (or H^{+} increases), chemical weathering at the surface of rock and soil particles occurs; this in turn mobilizes base cations and Al^{3+}; as previously mentioned, base cations are important for plant productivity and acid buffering, however, Al^{3+} is toxic to vegetation (Byers et al., 1938; UBA, 2004; Kochian et al., 2005).

1.3 DIGITAL SOIL MAPPING

Traditionally, mapping soils to understand their spatial distribution involved time-consuming and costly soil sampling which generally covered a minimal area, leaving knowledge gaps across large areas (McBratney et al., 2000). Born out of these constraints, the earliest form of kriging was developed and applied in the 1950's in the mining industry, when Danie Krige studied the most effective way to predict concentrations of high-grade gold ore based on the locations of known high-grade ore deposits. In the 1960's, Georges Matheron formalized the work of Krige, and presented it as the theory presently known as geostatistics (Babish, 2006). Geostatistics is a subset of statistics focused on the interpretation and analysis of data which is referenced geographically. Geostatistical techniques underpin predictive soil mapping, which use data sets with few soil observations, inexpensive information such as digital elevation models and remote sensing imagery, combined using geostatistical methods. These geostatistical methods included environmental correlation, and ordinary kriging, as well as hybrid methods such as regression kriging and kriging with external drift (Bishop & McBratney, 2001). In the digital mapping of soil properties, the conceptual model first introduced by Jenny (1941) is used, as the knowledge and understanding that *clorpt* factors influence soil properties is applied, and continuous maps of these factors can be used as predictors in order to create digital maps for soil properties in areas that have not been sampled. Using continuous maps in predictive digital mapping creates a conceptual difference from traditional soil mapping. Traditional soil maps used aerial photographs and Landsat images to define landscape features, which were used to generated subunits of soil types based on the soil surveyor's bias. The result was a soil map of 'polygons' which represented identified soil type

(Minasny and McBratney, 2015). In contrast, with continuous maps the coverage is not broken up into subunits, as such there are no obvious polygons or hard boundaries.

One of the most widely used methods for predictive soil mapping is regression kriging (RK) because of its flexibility in defining trends based on different linear models (Gasch et al., 2015). Regression kriging combines the regression of a dependent variable such as soil pH or Db on independent continuous auxiliary variables such as vegetation cover, temperature, and bedrock type with kriging of the regression residuals (Babish, 2006). Regression kriging has been found to be one of the most accurate methods for producing predictive maps for environmental factors (Bishop and McBratney, 2001). It should be noted that there are limitations to RK such as its complexity. Regression kriging, like all kriging methods, also completely relies on data quality and quantity. If data comes from different sources or the sampling design is not representative, and there are only a small number of sites (less than 50), then final predictions may be poor (Hengl et al., 2007). Considering these limitations, RK has still been found to be one of the most accurate methods for producing predictive maps for soils (Bishop and McBratney, 2001).

Historically, the emphasis of soil sampling and mapping has been on agricultural regions, with the aim to classify soils and improve our understanding of soil properties to support the continued development of the agricultural industry (Baldwin et al, 1938). Since the early 1980's, Agriculture and Agri-Food Canada has been producing national soil maps (Soil Landscapes Canada; SLC) and updating the accompanying database. The SLC is a product of the Canadian Soil Information Service (CanSIS); while it covers the entire nation, the focus has always been agricultural regions (Schut et al., 2011). However, the resolution for these maps is coarse (1:1,000,000), which can cause a generalization of map

features over such a large area (Schut et al., 2011). Unlike agricultural land, forest regions of Canada have not been highly sampled; the SLC database has only provided soil information for forested areas once, in the initial lunch of the project and has not been updated since. As well, the polygons found for the forest maps are large and imprecise (Schut et al., 2011). This has created a large knowledge gap, as Canada's forests comprise 10% of the worlds forest cover, and so it is important that their soil properties be better understood.

Digital mapping may close both of the knowledge gaps presented here; firstly, it can be applied to the agricultural areas where soil data already exists and can be used to improve the resolution for these areas. In addition, the vast area of forest in Canada is under sampled and has limited data, which has led to a minimal understanding of forest soil properties across the nations. Digital mapping is essential in these areas then, as it can be applied to the minimal data sets and produce digital soil maps which will increase this understanding.

1.4 KITIMAT, BRITISH COLUMBIA

The Kitimat Valley is located on the northwestern coast of British Columbia (BC) near the Pacific Ocean; its lowest point is at the head of the Douglas Channel in Kitimat to the south, and it stretches just past the city of Terrace, which is about 50 km to the north (ESSA et al., 2013). It is surrounded by mountainous coastal temperate rainforests and the landcover is dominated by dense forest, predominantly comprised of *Tsuga heteophylla* (Western Hemlock). The soils are typical of the coastal landscapes of forested Northern British Columbia; they are dominated by brunisols and podzols which have been formed on three main bedrock types: calc-alkaline volcanic rocks, granodioritic intrusive rocks and

quartz dioritic intrusive rocks. Soils have also been formed from glaciofluvial surficial materials as a result of glacial deposits (Clague, 1984; LNG technical data report; Stantec, 2014; Canadian System of Soil Classification, 1998). During the last decade, the increase in industry in this area and concern for pressures on the environment have resulted in several soil surveys of the Kitimat Valley such as the LNG technical report (Stantec, 2014), the sulphur dioxide technical assessment report (known as STAR from here on; ESSA et al., 2013) and Levasseur (2017). Through these surveys, soils have been analyzed for Db, field moisture, pH, exchangeable cations, OM, particle size, and major oxides; additionally, survey data was used to create a simple map of soil types. Lastly, mineral surface area and critical loads were estimated by Levasseur (2017), and STAR mapped critical loads (ESSA et al., 2013). However, fundamental physicochemical soil properties (e.g., Db, OM, CF, clay, pH, exchangeable acidity and exchangeable cations) have not been mapped for this region yet, so there is a limited understanding of their spatial variation in the Kitimat Valley. Mapping these soil properties is critical in order to manage the natural resources of the region, as well as identify any potential impacts industrial activity may have on the soil.

The population of Kitimat is small, with 6394 people based on the 2016 census, and the population of Terrance – which is the closest city to Kitimat – is 13,663 (Statscan 2016). While the region has a low population and is rugged and mountainous, it is still an area which has a considerable industrial influence, such as the Rio Tinto BC Works aluminum (Al) smelter, and the shipping of aluminum to markets in North America and Asia out of the Douglas Channel (ESSA et al., 2013). The construction of the Rio Tinto BC Works aluminum smelter (formerly known as Rio Tinto Alcan) began in 1951, and aluminum was first produced from the smelter in 1954. A modernization of the smelter was announced in

2006, called the Kitimat Modernization Project (KMP); the construction of this project began in 2011 and was completed in 2016. The modernization project increased aluminum production by 48% from its original capacity of 280,000 tonnes per year (t/yr). This increased production was accompanied by a permitted increase in sulphur dioxide (SO_2) emissions from 27 tonnes per day (t/d) to 42 t/d (ESSA et al., 2013). As there is a lack of soil maps and knowledge of the soil properties in the Kitimat valley, the potential impacts of sulphur (S) deposition from this smelter are unknown.

1.5 SOIL ACIDIFICATION

It is well established that metal smelters are large point sources of SO_2 emissions (Hutchinson and Whitby, 1977; Freedman and Hutchinson, 1980). Emissions of SO_2 have many pathways into the surrounding environment; once emitted, SO_2 can be transported in the atmosphere until it is removed via two processes: dry and wet deposition. Dry deposition occurs when gaseous SO_2 and particulate sulfate (SO_4^{2-}) are deposited directly onto the surrounding soil and vegetation as it is heavier than air and has a short residency time (1-3 days) in the atmosphere (Garland, 1977; Schwartz, 1989). Sulphur dioxide is deposited onto plant surfaces, where it is oxidized to SO_4^{2-} and washed off the forest canopy in rain events (Piirainen et al., 2002; Reuss and Johnson, 1986). Sulphur dioxide can also undergo oxidation in the atmosphere, ultimately resulting in the formation or sulphuric acid (H_2SO_4), which is deposited in rainfall (Kellogg et al., 1972; Mylona, 1996). Once this H_2SO_4 is deposited onto the earth's surface, it dissociates into H^+ and SO_4^{2-} (Guadalix and Pardo, 1991). As H^+ enters the soil, it binds preferentially to exchange sites where base cations (Ca^{2+}, Mg^{2+}, K^+, and Na^+) are displaced. As the concentration of H^+ increases with acidic deposition, more base cations are displaced from the exchanges sites in order to

neutralize the continued acidic deposition. If the amount of base cations in the soil is large enough to continually neutralize H^+ inputs, then the soil will not change; however, if the continued deposition is greater than the soils capacity to neutralize H^+, then the soil becomes acidified (van Breeman et al., 1984; Reuss and Johnson, 1986; Reuss et al., 1987; Fernandez et al., 2003). This acidification also influences metal toxicity, particularly Al^{3+}; when pH levels in soil are below 5, Al^{3+} becomes mobilized and is then bioavailable to plants. Aluminum is toxic to vegetation and may impact plant tissues through uptake from the root, or aquatic organisms in receiving waters when Al^{3+} is leached through the water table (Kochian et al., 2005). This in turn could cause a shift in plant populations to species which are more tolerant of acidic soil (Driscoll et al., 2001; Cape et al., 2003; Dore et al., 2007).

1.6 KEY SOIL PROPERTIES FOR MAPPING AND RISK ASSESSMENT

As previously described, soil quality, or the condition of a soil which can maintain a sustainable forest management, can be assessed by measuring physical and chemical soil properties such as Db, and soil particle size, OM, exchangeable cations, as well as pH. In order to manage forests of the Kitimat Valley, these soil properties need to be mapped because then the variation, magnitude and current state of these properties can be better understood. Once soil properties are mapped, they can also allow for the assessment of how sensitive the soils are to acidic deposition. Like soil quality, there are many soil properties which are used to assess soil sensitivity to acidic deposition. Risk assessments, such as the one completed by Williston et al., (2016) often evaluate the sensitivity of an area to acidic deposition through the calculation of critical loads. Critical loads in soils are defined as an estimate of exposure to a pollutant below a specified sensitivity to a chemical

criterion so that significant harmful effects on sensitive elements of the environment do not occur (Nilsson, 1988). More specifically, in the last 25 years, UNECE has been using critical loads of atmospheric nitrogen and sulphur as indicators of ecosystem sensitivity to acidification (UBA, 2004). Under the UNECE updated handbook for the Convention for Long-Range Transboundary Air Pollution (LRTAP; 2015), critical loads are defined as:

'[A] a quantitative estimate of the exposure to one or more pollutants below which significant harmful effects on specified sensitive elements of the environment do not occur according to present knowledge'

The chemical criterion chosen for critical loads is based on the dose response relationship between chemical characteristics and ecosystem functions. The critical criterion that has been used by UNECE is the aluminum to base cation ratio in the soil (Nilsson and Grennfelt, 1988). However, while critical loads are widely used in risk assessment, they produce steady-state quantities; this means that they do not include short-term buffering processes such as buffering via exchangeable base cations (Spranger et al, 2008). Soil properties such as cation exchange capacity (CEC), base saturation (BS) the base cation (BC) pools are three properties widely used as indicators of how well a soil may neutralize acidic deposition. These measures include short term buffers of acidic deposition and can ultimately lend an understanding to not just if an ecosystem is affected but when it could be affected. The CEC is the sum of the total amount of positively charged ions (called exchangeable base cations Ca^{2+}, Mg^{2+}, K^{+}, Na^{+}, and exchangeable acidic cations H^{+}, and Al^{3+}) bound on exchange complexes, or sites, found in the soil (Sonon, 2014). These soil exchange sites are the negative charges found on the surface of clay and organic matter particles. These negative charges attract Ca^{2+}, Mg^{2+}, K^{+}, Na^{+} because they

are positively charged, and so they adhere to the clay and organic matter particles where they are held in the soil and may be taken up by plants. As ions are constantly input into the soil through nutrient cycling, ions are continuously taken up and displaced; ions with higher valence (higher charge, like Ca^{2+}, Mg^{2+} and Al^{3+}) are preferentially bound to these sites (Reuss et al., 1987). The BS of a soil is the percentage of the CEC that is made up of the base cations Ca^{2+}, K^{+}, Mg^{2+}, and Na^{+} on the soil exchange sites (Shoenholtz et al., 2000). Lastly, BC pools are the total amount of base cations available in the soil at a given time; base cation pools are dependent on the base cation concentrations, soil bulk density, and the depth of soil being evaluated.

1.7 OBJECTIVES

The primary objective of this thesis was to assess the spatial variability of soil properties in the Kitimat Valley and create predictive soil maps for the region. Soil properties such as Db, OM, CF, clay, pH, exchangeable acidity, and exchangeable cations have not been previously mapped for this region; digital maps would allow for the understanding of the variation and state of these properties for the soils of this region.

The secondary objective of this thesis was to use predictive digital mapping in an application to assess the potential impacts of S deposition from the aluminum smelter in the Kitimat, Valley. To do this, first indicators of soil buffering capacity (CEC_E, BS_E, and BC pools) were evaluated to determine regional sensitivity to acidic deposition using predictive digital maps. These measures were used instead of critical loads because they provide a time to effects assessment where critical loads assessments focus on long-term impacts and ignore finite buffers such as BC pools. Secondly, the potential impacts to forest

soils in the Kitimat Valley was assessed using predictive digital maps of calculated time to base cation depletion.

To support this assessment, mineral soil samples were taken from 72 locations throughout the Kitimat region during the period 2012–2016 and were analyzed for Db, OM, CF, clay, pH, exchangeable acidity (H^+, Al^{3+}) and exchangeable cations (Ca^{2+}, Mg^{2+}, K^+, and Na^+). Predictive maps were created for these soil properties for the average of the top 50 cm of mineral soil using regression kriging following Hengl et al. (2004) and their quality was assessed. To assess the sensitivity of the soils, indicators of soil buffering capacity (CEC_E, BS_E, and total BC pools) were calculated. In addition, time to base cation pool depletion was calculated for the average of the top 50 cm of mineral soil using modelled S deposition based on permitted SO_2 emissions.

This thesis is written in manuscript style, divided into two main manuscript chapters to meet the overall objectives of this work. The first manuscript (Chapter 2) addresses the primary objectives, focusing on assessing the spatial variability of soil properties in the Kitimat Valley through the development of predictive digital maps for the region. Additionally, the quality of the predictive maps was assessed. The second manuscript (Chapter 3) addresses the secondary objectives, focusing on areas identified as sensitive to acidic deposition and assessing the potential impacts of increased SO_2 emissions through calculating the time to base cation pool depletion based on post-modernization total S deposition estimates. The description of the study region, sampling methods and sample sites are repeated across both chapters to facilitate stand-alone manuscripts.

2.0 CHAPTER 2: CHAPTER 2: PREDICTIVE MAPPING OF SOIL PROPERTIES IN THE KITIMAT VALLEY, BRITISH COLUMBIA

2.1 INTRODUCTION

Soil is a key natural resource which provides fundamental ecosystem services such as provisioning (i.e., agriculture, silviculture, and precious metals) as well as ecosystem regulation (water filtration and nutrient storage for plant productivity). These provisions are the backbone of the economic success of many countries; so, it is important then to understand the spatial patterns in soil properties to allow us to effectively manage these natural resources. Traditionally, mapping soils to understand their spatial distribution involved time-consuming and costly soil sampling which generally covered a minimal area leaving knowledge gaps across large areas (McBratney et al., 2000). Born out of these constraints, Danie Krige developed the earliest form of kriging for use in the mining industry; the location of high-grade gold was predicted based on the known locations of high-grade ore. In the 1960's, this work was formalized by Matherton, and presented as the theory known as geostatistics (Babish, 2006). Geostatistical techniques underpin predictive soil mapping, which use data sets with few soil observations, inexpensive information such as digital elevation models and remote sensing imagery, combined using geostatistical methods (Hengl, 2004). One of the most widely used methods for predictive soil mapping is regression kriging. Regression kriging combines the regression of a dependent variable such as soil pH or bulk density on independent continuous auxiliary variables such as vegetation cover, temperature, and bedrock type with kriging of the regression residuals (Babish, 2006). This method is used for predictive digital soil mapping because of its flexibility in defining trends based on different linear models (Gasch et al.,

2015). As well, it has been found to be one of the most accurate methods for producing predictive maps for environmental factors (Bishop and McBratney, 2001).

Globally, a shortage of soil maps has been documented; Grunwald and associates (2011) stated that soils are the least described spatial variable at the global scale, and that soil maps are often undocumented or incomplete. Digital soil mapping has been completed successfully in many cases worldwide; global maps for soil type at the 1 km scale (Hengl et al., 2014), as well as the 250 m scale for the continent of Africa (Hengl et al., 2017). These maps came from an initiative launched in 2009 called the *GlobalSoilMap* project after the second global workshop on Digital soil Mapping in 2006 (Hartemink et al., 2010). During this workshop, it was discussed and understood that maps of soil properties are not readily available; hence it was suggested that an initiative based on open source information and data contributed by many countries may allow for the creation of a global raster map of soil properties (Hartemink et al., 2010). Clearly, there has been some progress from this initiative, but for many areas, especially for areas such as Russia and Northern Canada, there is a serious knowledge gap. Hengl and colleagues (2014) acknowledged that these areas in particular lack the soil data required to complete reliable predictive digital mapping

The area of interest to this study is the Kitimat Valley, in North-West BC. There has been an increase in industrial activity in the Kitimat Valley in the last decade, and concern for pressures on natural resources, including soil, as a consequence of this industrial activity have resulted in the completion of several soil surveys in the region. Through these surveys, soils have been analyzed for bulk density, field moisture, pH, exchangeable cations, total organic carbon, particle size, and major oxides. Additionally,

mineral surface area and critical loads estimations were made by Levasseur (2017) and a simple map of soil types, as well as the exceedances of critical loads, were mapped by LNG Canada (Stantec, 2014) and ESSA et al., (2013) in the Sulphur dioxide technical assessment report (STAR). However, fundamental soil properties (e.g., Db, OM, CF, clay, and pH, exchangeable acidity, Ca^{2+}, Mg^{2+}, K^{+}, and Na^{+}) have not been mapped for this region yet, so there is a limited understanding of the spatial variability of these soil properties in the Kitimat Valley. Mapping these soil properties is critical in order to manage the natural resources of the region, as well as identify any potential impacts industrial activity may have on the soil.

The principle objective of this chapter was to predict soil properties (Db, OM, CF, clay, and pH, exchangeable acidity, Ca^{2+}, Mg^{2+}, K^{+}, and Na^{+}) across the Kitimat Valley through digital soil mapping. To do this, mineral soil samples at three fixed depths were taken from 72 locations throughout the Kitimat region during the period 2012–2016 and were analyzed for previously mentioned soil properties. Predictive maps were then created for these soil properties for the top 50 cm of mineral soil using regression kriging following Hengl et al. (2004) and their quality was assessed by calculating the total variation explained by the model (TVAR) and the normalized root mean square error (RMSE).

2.2 METHODS

2.2.1 STUDY AREA AND SITE SELECTION

The Kitimat Valley is located on the northwest coast of British Columbia; its lowest point (300 m) is at the head of the Douglas Channel close to the town of Kitimat, in the south of the valley, and the most northern point extends to just past the city of Terrace, which is about 50 km to the north (ESSA et al., 2013; Clague, 1984). Three bedrock types

are dominant in the region (calc-alkaline volcanic rocks, granodioritic intrusive rocks and quartz dioritic intrusive rocks); intrusive igneous rock has been shown to provide an acidic, coarse, parent material (Jenny, 1941). Additionally, surficial geology mapped and described by Clague (1984) showed that the valley bottom between Kitimat and Terrace was substantially covered by glacial deposits such as alpine complexes, till veneer, and glaciomarine sediments. This may be reflected in soil properties, as alpine complexes and till veneers can lead to the formation of more acidic soils (Tamminen and Starr, 1990), and glaciomarine sediments contain greater amount of base-rich minerals and produce soils with higher base cation weathering rates (Egli et al., 2001). Of the 10 soil orders found in Canada, there are three which are associated with forest landscapes: Luvisolic, Podzolic, and Brunisolic. Of these three soil orders, Podzolic and Brunisolic soils predominate the soil landscape of the Kitimat Valley (Canadian System of Soil Classification, 1998; LNG Canada, 2014). Soils of these orders are found in the same basic parent material type, often found in areas of sandy parent material underlain with igneous rock and areas of sandy glaciofluvial deposits. Podzols and Brunisols are found in the same parent material and are both found under canopies dominated by coniferous vegetation; however, they have fundamental differences. Podzols are acidic soils dominant in ecoregions with more than 700 mm of rain per year, where Brunisols are found in areas of less precipitation and are poorly weathered soils that lack distinct horizons which prevents them as being classified as podzols or luvisols. Podzols have a distinct light grey upper horizon that is formed from the increased precipitation and organic acids produced from the decomposition of coniferous leaf litter, which in turn creates a zone of strong weathering. This strong weathering causes eluviation, or the downward transport of primary minerals such as

aluminum, iron and other metal ions from the upper to lower horizons, thus the upper horizon is light (Canadian System of Soil Classification, 1998).

The Kitimat the Valley is located mainly within the Coastal Western Hemlock (CWH) biogeoclimatic zone, with the high elevation mountain regions being within the Alpine Tundra (AT) and Mountain Hemlock (MH) zones (Krajina, 1975). The CWH zone is on average the rainiest biogeoclimatic zone in British Columbia, with cool summers and mild winters (Meidinger and Pojar, 1991). This is true for Kitimat and Terrace, as the long-term (1981-2010) average yearly precipitation was 2774.6 and 1168.9 mm, and the annual average temperature was 7.9 and 7.4°C, respectively (Environment Canada, 2018).

The landcover in Kitimat Valley is dominated by dense forest, predominantly comprised of *Tsuga heteophylla* (Western Hemlock). The topography of the Kitimat Valley is very rugged, as it is flanked by mountain ranges with peaks as high as 1700 m. The principal industry in the region is the Rio Tinto BC Works smelter (ESSA et al., 2013). Also, a liquified natural gas (LNG) project in Kitimat has been announced recently, representing additional future industrial pressures on the surrounding environment. This LNG pipeline will carry natural gas to a processing facility in Kitimat where it will be condensed and shipped out of the Douglas Channel.

In the current study, the mapping domain was defined as a 3,000 km^2 rectangular area in the Kitimat Valley (see Figure 2-1) with an east-west dimension of 30 km and a north-south dimension of 100 km; this domain defines the area of potential anthropogenic impact from the smelter and related activities such as smelting, as well as accounts for potential future industrial activity which may also impact the area. To properly evaluate the impacts of these industries, soil samples were collected in this area. Site selection used

a stratified random sampling approach to ensure spatial coverage. The strata were based on the bedrock geology map for the study region, and within each stratum a minimum of 4 sampling sites were randomly selected. Soil sampling was carried out following a common protocol; a 500 by 500 m grid was overlaid on the study domain, and all accessible sites (within ~250 m from a road/trail) were identified; from this, sample sites were randomly selected. While sites were accessible, they were also more than 50 m away from roads, rivers, and lakes, were undisturbed by human activity, and have a slope of less than 45 degrees (ESSA et al., 2013). In addition, soil data were supplemented with samples from other surveys being carried out in the region; in total, soil samples at three fixed depths were taken from 57 locations. Lastly, in 2016, additional sites were sampled to supplement the spatial representation of sites collected in 2012 (n=15). A total of 72 locations were sampled following a common sampling protocol during the period 2012–2016 (see Figure 2-1). For details on locations and site characteristics, please see Appendix Table A1.

Figure 2-1. Spatial coverage of the 72 soil sampling locations within the Kitimat Valley. Samples were collected during 2012 and 2016; the blue dots represent a single sample location.

2.2.2 FIELD PROCEDURES

At each sampling location, after the 20 m by 20 m plot was established, the sample field-sheet was filled out, where observations such as site ID, co-ordinates, time, date, temperature, elevation, site position, slope, and dominant vegetation were recorded. Then, at each of the four corners and the centre of the plot, a soil auger was used to collect mineral soils from the fixed depths of: 0-10 cm, 15-25 cm, and 40-50 cm (below the forest floor); the five samples from each respective depth were then composited into one sample per depth and labeled accordingly (making a total of three depth samples per plot). These three samples were taken to provide a representative average for the top 50 cm of soil. In addition, soil bulk density samples were collected from the centre of the plot using a hammer core, at the same depths as the composite soil samples. Samples were retaken in the presence of large rocks and roots; after sampling, each of the bulk density samples were

place in their own plastic bags and labeled (ESSA et al., 2013). In total, 72 sites were sampled throughout the Kitimat Valley between 2012 and 2016 using this field protocol. The total number of individual soil samples collected for chemical analysis was 213 samples (depths 15-25 were missing for three sites: GD009, OG009, and VA002), which were sent to Trent University for preparation and laboratory analysis. For a complete table of site coordinates and characteristics, see Appendix Table A1.

2.2.3 LABORATORY METHODS

Upon arrival in the laboratory, all bulk density and composite samples were weighed, then composite samples were transferred into aluminum foil pans, and allowed to air dry for 2 weeks. Samples were then sieved in a 2 mm sieve and the coarse (> 2 mm) and fine (< 2 mm) fractions were weighed.

All soils (n=213) were analyzed for Db, OM by loss on ignition, CF (> 2 mm), pH, and particle size (sand, silt and clay), following the methods outlined by ESSA et al. (2013). All samples were analyzed for exchangeable cations (Ca, K, Mg, Na, Fe, Mn) following Dohrmann et al. (2012), exchangeable acidity and aluminum (Al^{3+}) following Thomas (1982) and Sims (1996).

Coarse fragment and bulk density (Db)

All Db samples were oven dried at 105°C for 24 hours; dried samples were then sieved in a 2 mm sieve, and the coarse (>2 mm) and fine (<2 mm) materials were weighed.

The volume of coarse fragment (>2 mm), was estimated by adding the sieved coarse fragment (> 2 mm) to 100 mL of water in a graduated cylinder and recording the volume of water that was displaced.

Db was calculated according to the equation:

$$Bulk\ density\ (g\ cm^{-3}) = \frac{Dry\ weight\ of\ fine\ (< 2\ mm) fraction\ (g)}{Soil\ core\ volume\ (cm^3) - Coarse\ fraction\ displacement\ (cm^3)}$$

Where the soil core volume was the volume of the bulk density hammer ring used in the field.

pH, organic matter, and particle size

Upon arrival to the laboratory, a 10 g subsample of fresh soil was taken for pH analysis before the remaining sample was air dried. Soil pH was measured in water; fresh soil was sieved (< 2 mm) to remove coarse debris, and 5 g was weighed out into a labeled conical tube. Then 20 mL of b-pure water was added, and samples were placed on a shaker table for 40 minutes. After being shaken, they were left to sit for 20 minutes to allow the particles to settle. A glass-probe pH electrode calibrated using 3 pH standards was used to record the pH. The pH probe was rinsed with b-pure water between samples to avoid cross contamination.

Sample crucibles were washed with DI water, oven dried at 105°C for 3-4 hours until all moisture was removed and placed in a desiccator to cool. Empty crucibles were then labeled with ink and weights were recorded using an analytical balance; approximately 5 grams of fine air-dried soil (<2 mm) was then added to the crucible. Full crucibles were oven dried for 12 hours at 105°C, transferred to a desiccator and dried weights were recorded. Finally, the full crucibles were placed in a muffle furnace and ignited (ashed) at 400°C for 10 hours. After cooling in a desiccator, final weights were recorded. From this, percent organic matter was calculated using the following formula:

$$\%OM = \frac{(weight\ of\ dry\ soil - \ weight\ of\ ashed\ soil)}{(weight\ of\ dry\ soil)} * 100$$

All samples were analyzed for particle size using laser diffraction (Horiba Partica LA-950) following methods outlined by Whitfield and Reid (2013). Samples were dried, sieved, and run in triplicate; the different size particle fractions were identified, and grouped by sand (60-250 µm), silt (2-6 µm) and clay (< 2 µm) size categories. The average of the triplicates was then used to describe the percent of sand, silt, and clay.

Exchangeable cations and exchangeable acidity

Exchangeable cations were determined for all soil samples using an ammonium acetate (NH_4OAc) extraction, following protocols outlined by Dohrmann et al. (2012). One litre of 1 M NH_4OAc solution was made by adding 77.08 g of NH_4OAc to 1 L of b-pure water and adjusting the pH to 7 by adding ammonium hydroxide (NH_4OH) or acetic acid (CH3COOH). Five grams of air-dried soil was weighed into a labeled 50 mL conical tube, and 25 mL of NH_4OAc was added. The samples were shaken for 15 minutes and then allowed to stand for approximately 16 hours. A Buchner funnel was fitted with #42 Whatman filter paper and placed on a 250 mL Buchner flask with a vacuum side arm and rubber ring, ensuring a proper seal. The vacuum filter was turned on, and the filter paper moistened to ensure suction. The soil was transferred from the conical tube to the Buchner funnel, and washed twice with 10 mL of NH_4OAc, allowing each wash to go through the funnel without the soil cracking and drying out. The extractant was poured into a labeled 50 mL conical tube. A subsample was then acidified with nitric acid (HNO_3; 2% by volume) and analyzed for cations (Ca^{2+}, Mg^{2+}, K^+ and Na^+) using inductively coupled

plasma optical emission spectrometry (ICP-OES; Optima 7000DV). A total of 18 method blanks were analyzed, as at least three blanks were included in each batch of 50 samples. These method blanks were then used to blank correct the analysis. Additionally, Buchner funnels were washed 3 times with 10 mL of b-pure water between samples to ensure accurate and reliable analysis.

Soil samples were analyzed for exchangeable acidity following the methods outlined by Thomas (1982) and Sims (1996). Potassium chloride (KCl; 1M) and sodium hydroxide (NaOH) solutions were made. The NaOH solution was then titrated with standardized hydrochloric acid (HCl) three times and the concentration of the NaOH solution was verified to be ~0.1 N using the formula:

$$C_1V_1 = C_2 V_2$$

Five grams of air-dried soil was weighed into a labeled 50 mL conical tube; 25 mL of 1 M KCl solution was added and the mixture was left to sit for 30 minutes. A Buchner funnel was fitted to a 250 mL flask with a vacuum side-arm and #42 Whatman filter paper. Light suction was applied, and the filter paper was moistened; the soil-KCl mixture was then transferred to the Buchner funnel. The soil was washed with an additional 125 mL of KCl solution in increments of 25 mL, ensuring the solution ran through the filter but the soil was not dried or cracked. A subsample of leachate (15 mL) was poured into a conical tube and acidified with HNO_3 (2% by volume) for analysis of Al by ICP-OES (Optima 7000DV). The remainder of the extractant (135 mL) was used to obtain exchangeable acidity; to do this, 4–5 drops of phenolphthalein were added to the leachate in the 250 mL flask and titrated with the 0.1 N NaOH to the first permanent pink point. Volumes of NaOH

were recorded before and after titration, and total volume was used to calculate exchangeable acidity. A total of 30 method blanks were analyzed during this procedure, as at least three method blanks were run for each set of 25 samples to allow for blank correction. Buchner funnels were washed 3 times with b-pure water between samples to ensure accurate and reliable analysis.

2.2.4 DESCRIPTIVE SUMMARY OF SOIL DATA

Summary statistics (minimum, maximum, and average), as well as coefficient of variation (CV%) were calculated for the 0-10, 15-25, and 40-50 cm depth data. The CV was calculated using the formula:

$$CV\% = \frac{\text{standard deviation}}{mean} * 100$$

The data distribution for each soil variable was visually assessed using boxplots and tested for normality using the D'Agostino-Pearson Test. Finally, the Kruskal-Wallis test was used to determine if there were statistical differences in soil variables between depths; a Dunn's test was used post-hoc to determine which depths were statistically different.

2.2.5 PREDICTIVE MAPPING PROCEDURES

Predictive mapping using regression kriging followed the generic framework outlined by Hengl et al. (2004; Figure 2-2). (1) covariate layers (independent variables or predictors such as factors which affect soil formation (*clorpt*) see Table 2-2; full list in Appendix Table A2) were prepared in QGIS. (2) the dependent, or target variables (soil properties; Db, OM, CF, clay, pH, exchangeable acidity, Ca^{2+}, Mg^{2+}, K^{+}, and Na^{+}) were transformed, and the RK, fitting semivariograms, as well as the back transformation of the

predictive models were all carried out using Statistical software packages in R (Global Soil Information Facilities (GSIF), raster, sp, rgdal, and gtools, boot, factoextra, corrplot, HydroGOF). (3) predictive maps were visualized in QGIS. This predictive mapping procedure was performed for soil properties (Db, OM, CF, clay, pH, exchangeable acidity and exchangeable cations) for the average of the top 50 cm of mineral soil.

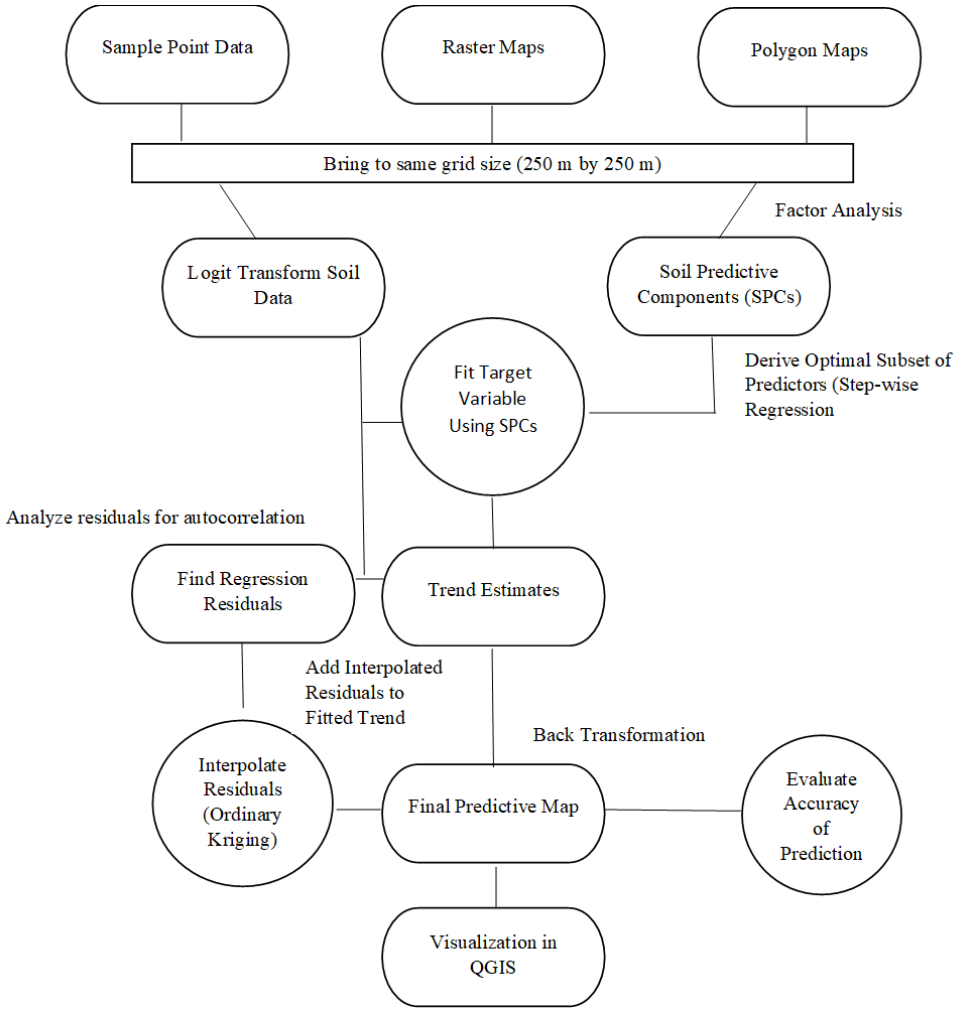

Figure 2-2 The generic framework outlined by Hengl et al. (2004), adapted for use in this study.

Preparing Covariates

The first step to producing predictive maps for the soil properties (Db, OM, CF, clay, pH, exchangeable acidity and exchangeable cations) for the study area was to unify the projections and the grid size of the covariate (auxiliary) maps. Covariates are the

independent variables, such as elevation, temperature, slope, and forest vegetation, which have continuous coverage across the study area. In total, 91 covariates maps were prepared, the categories of maps were: elevation, slope, geology, forest cover, precipitation, runoff, and temperature (Table 2-1, Table A2). Geology and forest cover covariate layers were chosen based on their presence in the study domain; if a geology or vegetation type was present in any part of the study domain, it was included. All covariate maps were unified to the Statistics Canada Lambert, EPSG 3347 projection; this projection was used as it produces less distortion for north western regions of Canada. All covariate maps were converted into raster maps with a 250 m × 250 m grid spacing over the study domain, e.g., vector data, such as geology, were rasterized (using the *rasterize* tool in QGIS version 2.18). This grid spacing was selected because 68 of the 91 covariate maps had a 250 m by 250 m grid spacing when retrieved from their respective sources, so all others were adjusted to match that grid spacing. Once grid spacing and projection were the same, the 91 rasterized covariate maps were compiled into a "raster stack" using the *stack* package in R. This raster stack was then transformed into factors, referred to as soil predictive components (SPC's), which are derived from principle component analysis (PCA) using the GSIF R package. SPC's are used in predictive mapping instead of the original predictor (auxiliary) values because it removes skew and covariance between the variables (Hengl et al., 2004). A scree plot was used to determine how many SPC's were used in the predictive mapping; a scree plot shows what fraction of the total variance is explained by the SPC's.

Table 2-1 Covariate data for predictive mapping: data type (climate, soil, hydrology, topography, geology, and forest vegetation; as well as the number of maps from each category), variable, data (map) resolution and source.

Data type	Variables	Resolution	Source
Climate (n = 15)	Total precipitation, annual mean, maximum and minimum temperature	10 km grid	Canadian Forestry Service; (McKenney, 2006)
Soil (n = 30)	Bulk density, cation exchange capacity, percent clay, coarse fraction volume, organic carbon, pH, percent sand, soil type	250 m	SoilGrids; (www.soilgrids.org)
Hydrology (n = 1)	Runoff (Q)	250 m	Cubic spline interpolation at 250 m of meteorological data from 16,115 points produced by the MetHyd model (New et al., 2000; Bonten et al., 2016)
Typography (n = 2)	DEM, slope	30 m	Canadian Digital Surface Model; (https://open.canada.ca/data/en/dataset/768570f8-5761-498a-bd6a-315eb6cc023d)
Geology (n = 6)	Bedrock type	Vector data, bedrock units	British Columbia Geological Survey (Cui et al., 2017)
Forest Vegetation (n = 37)	Vegetated and non-vegetated landcover, species composition, forest structure	250 m	Canada's National Forestry Inventory (Beaudoin et al., 2014)

Transform Target Variables and Perform Regression Kriging to Produce Predictive Models

Observed soil data by depth (Db, OM, CF, clay, pH, exchangeable cations, Ca^{2+}, Mg^{2+}, K^{+}, and Na^{+}) were averaged (weighted by bulk density and depth) so that the target variables represented the average top 50 cm of mineral soil. Predictive mapping was then carried out on this 0–50 cm soil depth.

The GSIF package was used to automate the methods involved in regression kriging. Each target variable was logit transformed; logit transformation is a function that log transforms a dataset, which is bound by a specified minimum and maximum and improves the normality of target variables (Hengl et al., 2007). The logit transformed data was then fit with the SPC's produced from the covariate layers, using the *fit.gstatModel* function in GSIF. This function uses stepwise regression to derive the best set of predictors based on Akaike Information Criterion (AIC) scores, which are then used to fit the target variables with a general linear model (GLM) (Hengl et al., 2004). After the data is fit with the GLM, the *fit.gstatModel* function performs the kriging of the regression residuals; these interpolated residuals are then added to the fitted GLM and a final prediction map is created.

Once the predictive maps of the target variables are produced, they are back transformed from the logit scale to the original units of the target variables using the *inv.logit* function from the *boot* package; this back transformed map was then imported into QGIS for final visualization.

Lastly, it should be noted that rare high values (outliers) were assessed using Cook's distance and Q-Q plots produced in R. In extreme cases, these rare high values were removed when interpolation was improved, or where all values remained inside of cook's distance and TVAR and RMSE increased.

2.2.6 STATISTICAL ANALYSIS AND VALIDATION OF PREDICTIVE MAPS

Using the *GSTAT* package and *krige.cv* function in R, a five-fold cross validation was run on the 72 observed data points after the predictive mapping procedure was completed; this function splits the observations up into N parts as specified by the user,

and predictions are made on N-1 parts. In this case N=5; this means the data were broken up into groups of 14-15 points each (each of these groupings is then called a fold). To run cross-validation, one group of 14-15 observations is left out, and the 57 or 58 observations are used to predict this smaller group. These predictions are run a total of 5 times, once for each group of 14-15 points (or fold) which have been left out; the *krige.cv* function runs 5-fold validation as the default (Pebesma, 2004). The cross-validation was then used to calculate the total variation (TVAR) explained by the model (TVAR, GSIF package; Hengl et al., 2013). TVAR is calculated using the following equation:

$$TVAR = \left[1 - \frac{SSE}{SSTO}\right] * 100\%$$

Where SSE is the sum of squares for the residuals at cross-validation points and SSTO is the total sum of squares (Hengl et al., 2014).

Cross-validation was also used to create predicted versus observed plots which were used to visually assess the goodness of fit of the predictive models created with the whole dataset. Additionally, normalized RMSE (NRMSE) was calculated in R using the *rmse* function of the *HydroGOF* package and normalized by dividing by the mean. This was done to assess the difference between the predicted versus observed data at the 72 sample locations.

2.3 RESULTS AND DISCUSSION

2.3.1 OBSERVED SOIL DATA

Average Db, coarse fragment, and pH increased with increasing depth (0-10, 15-25, 40-50 cm; Table 2-2; Appendix Figure A1). Average Db by depth was 0.59 (0.09-1.19), 0.75 (0.09-1.39), and 0.83 (0.13-2.00) g/cm^3. Average CF was 14.98 (0.00-80.61), 18.51 (0.00-93.68), and 21.43 (0.00-65.91) %. Average pH was 4.6 (3.7-6.5), 5.0 (4.0-6.6), and

5.3 (4.71-6.6). In contrast, average OM, clay, exchangeable acidity, and Ex. K^+ decreased with depth (Table 2-2; Figure A1). Average OM was 17.53 (2.60-89.48), and 12.62 (1.94-52.78) and 8.85 (1.81-61.67) %. Average Ex. acidity was 3.95 (0.13-15.13), 2.77 (0.53-8.53), and 2.04 (0.13-8.60) meq/100g. Exchangeable K^+ had average values of 0.16 (0.02-0.83), 0.11 (0.02-0.41), and 0.10 (0.45) meq/100g.

The increase in Db and pH with increase in depth was in line with previous literature; Db in soils typically increases with soil depth, as deeper soil layers contain less OM, are more compacted and have less root penetration than surface layers (Larson and Pierce, 1991; Doran and Parkin, 1994). Similarly, a previous study has also shown that pH increases with depth; especially for soils under forest canopy (Dorji et al., 2014).

The decrease in Ex K^+ with depth is widely observed (Giehl and Wiren, 2014). Exchangeable K^+ may have less vertical movement through soil because it is found at lesser concentrations than other exchangeable base cations; Ex. K^+ has been found at concentrations 10 times lower than Ex. Ca^{2+} and half of Ex. Mg^{2+} (Brady, 1984). As there is less Ex. K^+ in the soil and available for plant growth, it is often found that plants do not release Ex. K^+ back into the soil, and so they become reservoirs. This is opposed to abundant cations like Ex. Ca^{2+}, which shows a consistent pattern of nutrient cycling – it is taken up by plants and returned to the soil through leaf-litter fall – contributing to consistency in concentration with depth (Likens et al., 1967; Brady, 1984; Likens et al., 1994). Jobaggy and Jackson also found that like the current study, OM and clay decrease with depth globally in soils (2000).

The CV% by depth showed high ranges for many of the soil properties, with only Db showing less than 50% (Table 2-2). However, many of the soil properties showed a

decrease in the coefficient of variation with an increase in depth; for example, coarse fragment, clay, and pH all decreased in CV% with an increase in depth (Table 2-2). These CV values indicate that the spatial variation of the soil across the region changes by depth. The largest decreases were observed for coarse fragment (120.5, 101.2, and 88.4%), clay (105.2, 76.2, and 74.1%), and pH (162.3, 142.5, and 92.8%; note minimum, maximum, average, and CV for the log $[H^+]$ values were calculated first and then converted back to pH) (Table 2-2).

The high coefficient of variation indicated high spatial variation within the data over the study area; factors of soil formation such as slope, and type of parent material may explain this variation; slope may have affected the variation, as it was found by Moore et al. (1993), that terrain attributes such as slope were significantly correlated to soil properties such as clay and pH. Additionally, slope can influence erosion and transportation of materials from higher elevation areas to flatter plains (Marbut, 1935). This would be the case in the Kitimat Valley, as it is surrounded by mountains, and so material may have been eroded from the mountainous areas and transported to the glacial outwash plains. Parent material is a major factor for the formation of soil and its inherent properties such as texture, acidity, and nutrient density (Anderson, 1988; Osher and Buol, 1998; Brady and Weil, 2010). This is not true for a proportion of the Valley though, as surficial materials such as glaciofluvial surficial deposits, covered 26% of the study area. Glaciofluvial materials dictate the weathering of cations rather than bedrock geology or parent material in these soils; areas dominated by glaciofluvial deposits may have higher base rich minerals and may show different properties that would be expected from the bedrock geology (Egli et al., 2001).

Soil Db, OM, pH, Ex. acidity, and Ex. K^+ were found to have significant differences between depths ($p<0.05$, Table 2-3). Although Ex. Mg^{2+} did not show a consistent increase or decrease with depth it was found to have a significant difference between the upper and lower soil depths (Table 2-3). Soil Db, Ex. acidity, and Ex K^+ were significantly different between the 0-10 and 15-25 cm layers (Table 2). Further, Db, OM, pH, Ex. acidity, and Ex. K^+ all showed a statistical difference between the 0-10 and 40-50 cm layers (Table 2-3). A significant difference between the 0-10 and 40-50 cm depths was expected because of soil processes and biological factors which dictate the distribution of soil properties. Leaching, evaporation, nutrient uptake and decomposition facilitated by vegetation and earthworms all occur at the upper layers of soil and decrease with depth. This is especially true for the exchangeable cations, of which many are required for plant growth (Jobaggy et al., 2001; Giehl and Wiren, 2014). As well, upper soil depths contain more organic matter owing to litter fall, which can affect soil nutrient availability, soil texture, and soil density. This is opposed to lower soil depths which have less organic matter and are more compact, creating a more uniform soil which ultimately is less variable than the upper depths (Shoenholtz et al., 2000).

Table 2-2 Average soil properties (bulk density, coarse fragment, organic matter, clay, exchangeable [Ex] acidity and Ex cations) and coefficient of variation (CV; %) at three sampling depths (0-10 cm, 15-25 cm, and 40-50 cm) for all 72 sampling locations in the Kitimat Valley, British Columbia.

Parameter	Units	Average by soil depth			CV% by soil depth		
Soil depth	cm	0-10	15-25	40-50	0-10	15-25	40-50
Bulk density	g/cm3	0.59	0.75	0.83	48.58	37.05	46.48
Coarse fragment	%	14.89	18.51	21.43	120.47	101.24	88.4
Organic matter	%	17.53	12.62	8.85	94.18	81.86	97.10
Clay	%	4.93	4.51	4.04	105.24	76.20	74.09
pH (H_2O)		4.6	5.0	5.3	162.25	142.50	92.78
Ex acidity	meq/100g	3.95	2.77	2.04	64.32	65.36	81.06
Ex calcium	meq/100g	1.92	1.43	1.78	128.01	153.09	138.92
Ex potassium	meq/100g	0.16	0.11	0.10	78.96	70.35	82.98
Ex magnesium	meq/100g	0.50	0.31	0.43	114.62	127.75	175.93
Ex sodium	meq/100g	0.08	0.06	0.10	218.24	184.89	300.96

Table 2-3 Dunn's tests (Significance at $p<0.025$, indicated by *) for all significantly different soil properties (bulk density, coarse fragment, organic matter, clay, exchangeable [Ex] acidity and Ex cations) and coefficient of variation (CV; %) comparing the three sampling depths (0-10 cm, 15-25 cm, and 40-50 cm) for all 72 sampling locations in the Kitimat Valley, British Columbia.

		0-10 cm vs 15-25 cm	0-10 cm vs 40-50 cm	15-25 cm vs 40-50 cm
Parameter	Units			
Bulk density	g/cm3	*	*	
Coarse fragment	%			
Organic matter	%		*	*
Sand	%			
Silt	%			
Clay	%			
pH (H_2O)			*	
Ex acidity	meq/100g	*	*	
Ex calcium	meq/100g			
Ex potassium	meq/100g	*	*	
Ex magnesium	meq/100g	*	*	
Ex sodium	meq/100g			
Ex aluminum	meq/100g			
Ex iron	meq/100g			
Ex manganese	meq/100g		*	

2.3.2 OBSERVED SOIL DATA: WEIGHTED-AVERAGES

In general, the weighted-average soil properties for the 0-50 cm soil depth were very similar to the 15-25 cm layer (Table 2-2, Table 2-4). The weighted average for bulk density was 0.74 g/cm^3, with a range of 0.12-1.47 g/cm^3 (15-25 cm layer average: 0.75 g/cm^3). The weighted averages for pH was 5.01 and a range of 4.33-6.48 (15-25 cm: 5.0); and exchangeable acidity was 2.58 meq/100g with a range of 0.13-6.89 meq/100g (15-25 cm: 2.77 meq/100g). In contrast, the weighted average of exchangeable calcium and magnesium were similar to the 40-50 cm layer. Exchangeable calcium had a weighted average of 1.72 meq/100g and a range of 0.04-11.36 meq/100g (40-50 cm: 1.78 meq/100g); exchangeable magnesium had a weighted average of 0.40 meq/100g and a range of 0.02-3.42 meq/100g (40-50 cm: 0.43 meq/100g).

The CV% for the weighted averages of bulk density, coarse fragment, organic matter, exchangeable acidity, and potassium were lower than the CV% for the individual soil depths (38.5, 85.1, 69.9, 59.8, and 69.1%, respectively; Table 2-2, Table 2-4). The soil properties with the highest CV for the weighted averages were sodium (261.1%), magnesium (136.8%), calcium (132.7%), pH (117.5%) and clay (100.5%). These high CV values indicated that these properties were highly variable across the study area. Also, the CV values for the top 50 cm of mineral soil for these properties for were not always lower than the CV values of the individual observed soil depths of 0-10, 15-25, and 40-50 cm (Table 2-2, Table 2-4).

Lower variation found in the weighted soil depth is likely caused by how the weighted soil depth is calculated; the lowest depths generally had the highest bulk density, and so had the greatest weighting of the three depths. This is because at lower depths, where bulk

density is higher, there is more soil, which therefore represents more of the available nutrient reservoirs. This is congruent with what Geisler and Lundstrom (1993) found, which was that bulked soil samples showed reduced variation for cations such as sodium, magnesium and potassium when compared to individual soil samples.

Table 2-4 Minimum, maximum, average and coefficient of variation (CV; %) values of soil properties (bulk density, coarse fragment, organic matter, clay, exchangeable [Ex] acidity and Ex cations) of the top 50 cm of mineral soil for all 72 sampling locations in the Kitimat Valley, British Columbia.

Parameter	Units	Minimum	Maximum	Average	CV%
Bulk density	g/cm3	0.12	1.47	0.74	38.5
Coarse fragment	%	0.05	80.61	19.45	85.1
Organic matter	%	2.33	36.29	11.28	69.9
Clay	%	0.85	37.40	4.77	100.5
pH (H_2O)		4.33	6.48	5.01	117.5
Ex acidity	meq/100g	0.13	6.89	2.58	59.8
Ex calcium	meq/100g	0.04	11.36	1.72	132.7
Ex potassium	meq/100g	0.02	0.39	0.12	69.1
Ex magnesium	meq/100g	0.02	3.42	0.40	136.8
Ex sodium	meq/100g	0.00	1.65	0.08	261.1

2.3.3 PREDICTOR VARIABLES, EVALUATION OF FIT, AND DIGITAL SOIL MAPS

The scree plot showed that most variation was explained by the first 10 SPC's (Figure 2-3), to further investigate the predictors which were included in these 10 SPC's, an SPC contribution map was made (see Appendix Figure A2). Here it was seen that the first 20 SPC's had some of the strongest predictor variables, and so a total of 20 SPC's were used.

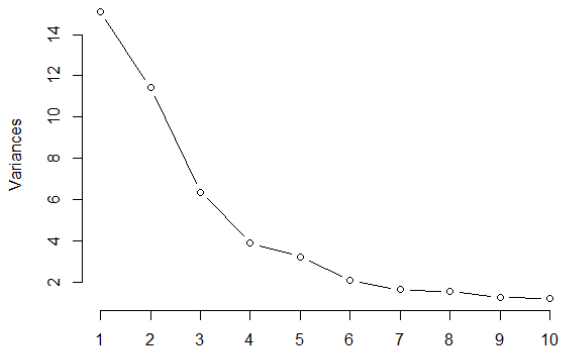

Figure 2-3 Scree plot, with SPC's (principal components) 1-10 compared to the variance (%) explained by each individual SPC.

The SPC contribution map showed distinct groupings of predictors; climate variables were shown to have the greatest contribution of all the independent variables to the SPC (Appendix Figure A2). After climate, soil properties (i.e., coarse fraction volume and percent sand) and bedrock type, showed to have contributed moderately. Climate is a factor of soil formation, and bedrock is the precursor for parent material which is another soil formation factor; Jenny (1941), stated that climate and parent material were the two most influential factors in terms of soil formation (Jenny, 1941). As such, it would make sense that these two factors had a higher contribution to the SPC than all other factors. All species of hemlock, which included: *Tsuga heteophylla*, *Tsuga canadensis*, *and Tsuga mertensiana*, (Western, Eastern, and Mountain hemlock) were included as predictors, however, only Eastern and Western hemlock showed any contribution to the SPC, which was found to be weak (Appendix Figure A3). It is unsurprising that Western Hemlock contributed to the SPC, as it is the dominating vegetation cover in the study domain (ESSA et al., 2013).

The comparison of predicted against observed for Db, OM, CF, pH (H_2O), and exchangeable Ca^{2+}, Mg^{2+}, K^{+} were clustered around the 1: 1 line suggesting a strong

goodness-of-fit (Figure 2-4). The strong spatial relationships for Db, CF and exchangeable Ca^{2+} were reinforced by their respective semivariograms (Appendix Figure A4), which showed a closer distance between the residuals and a better model fit. Additionally, the TVAR for these soil properties were found to be the highest for Db, OM, CF, pH, and exchangeable Ca^{2+}, Mg^{2+}, K^{+}, with values of 19.8, 26.4, 21.2, 24.3, 17.7, 21.0, 27.2% respectively (Table 2-5). While the goodness of fit was strong for organic matter, the semivariogram showed no distinct model fit (Appendix Figure A4; Table 2-5). Clay, exchangeable acidity, and Na^{+} had an almost horizontal spread in the predicted values versus the empirical data (Figure 2-5), indicating a poor fit of the regression relationship and residuals (Appendix Figure A4). However, only the semivariogram for clay reinforced the poor spatial relationship. The total variation explained for clay, exchangeable acidity, and sodium were low, at 0, 11.5, and 2.5% (Table 2-5).

Low TVAR values such as the ones seen in this study were also seen in a global study, where RK was applied for mapping soil properties (soil organic carbon, pH, sand, silt, clay, Db, CEC, and CF) at a 1 km grid spacing. The TVAR calculated for their soil properties ranged from 23-51% in this study and rarely exceeded 50% (Hengl et al., 2014). This being said, it was suggested that low TVAR values may be improved upon by using more sophisticated geostatistical methods, such as machine learning and random forest models, but these techniques also come with their own drawbacks, such as overfitting of the predictor variables (Hengl et al., 2014). As well, as discussed above, the predictor variables have uncertainties which may affect variation; as predictor data continues to be collected and improved, the databases will be improved, which will ultimately improve the quality of the maps.

The Db, OM and exchangeable K^+ had NRMSE values of 35.0 and 37.0, and 58.0% (Table 2-5), which were generally consistent with total variation explained by the models (Table 2-5). Additionally, Hengl (2007) stated that an NRMSE value close to 40% is generally satisfactory in terms of prediction; this means that the mapping of Db and OM were the most successful of all soil properties. The NRMSE for CF, pH, exchangeable Ca^{2+} and exchangeable Mg^{2+} were found to be higher at 132, 194, 157, and 130% (Table 5). An NRMSE value of >70% is typically qualified as less satisfactory (Hengl, 2007). The NRMSE value for exchangeable acidity was low (56.0%) compared to TVAR explained by the model (Table 2-5). Exchangeable Na^+ and clay had lower NRMSE values (63.0 and 61.0%), which are generally satisfactory but were not supported by their very little to no TVAR values. This could be because the range in values seen in the observed data for these properties is not as wide as the others, such as CF, which had a high range in values (Table 2-4). As digital mapping relies on the variation of the observed data to predict unknown areas, if the values have a smaller range and are very similar, it may be more difficult to estimate trends, resulting in a final map with a low TVAR value.

Based on the TVAR values for the soil properties evaluated in this study, the predictive maps can be ranked by the confidence in which they were mapped. Soil properties were found to be mapped with acceptable confidence with the exception of clay, which was not mapped acceptably. The order of confidence for the soil properties was: Ex Mg^{2+} > OM > pH > CF > Ex K^+ > Db > Ex Ca^{2+} > Ex acidity > Ex Na^+.

Before moving on to the visualization of the maps, it should be noted here the cross validation used to estimate the TVAR values was based on N=5 number of groups. This was based on a previous study which suggested that N=5 or N=10 should be used in model

training because there is a bias-variance trade-off; having more folds (smaller groups) leads to less prediction bias but has higher amounts of predicted variance (James et al., 2013). Ideally, a dataset is large enough that a validation set – or randomly selected data points, which are not used to create the model – would be used to validate the model rather than cross validation. Validations sets are used because they eliminate any bias that may be found when using cross-validation, as comparing any data to itself will cause some degree of bias (James et al., 2013).

Visually, the predictive maps for the top 50 cm of mineral soil indicated lower values in the glacial outwash plain compared with mountainous upper region and sloped sides of the valley for CF, OM, exchangeable acidity, K^+, and Na^+ (Figure 2-5). In contrast, Db, clay, pH, exchangeable Ca^{2+}, and Mg^{2+} all showed patterns of higher values in the bottom of the valley in comparison to the mountainous and sloped regions (Figure 2-5).

When discussing these digital maps, it would be remiss not to discuss their uncertainty and reliability, as the uncertainty in the maps used to predict soil properties may affect the variation of the final digital maps produced. Five main sources of uncertainty in digital maps have been identified by Finke (2006). First was positional accuracy, which is whether map boundaries are correctly aligned; raster maps must be aligned in a raster stack and the boundaries the same, in order to perform RK. Secondly, completeness of the dataset (both in analysis and geographically for the study domain); in this study, it may be that the south-western corner had less samples than the rest of the study area, and therefore may have been inaccurately fit, there are limited samples surrounding it to estimate from. As well, the errors associated with the measurements of soil analysis were identified by Finke (2006); data retrieved for digital soil mapping is

completed by many individuals, and errors in their measurements may not be identified prior to using the data for predictive mapping. Lastly, how up to date the data is and its lineage (when maps of different scales and data sources are combined) were determined to be sources of uncertainty in continuous soil data and digital maps. Specifically, lineage was an issue covariate map for soil type, as maps of different scales and data sources were combined to create it (Omuto et al., 2012; Grunwald et al, 2011).

While not all the maps have reached the level of confidence as previously found in the literature, there is no doubt that they are a helpful tool in which the soil properties of the area can be assessed. Based on the current trends in soil mapping, predictive digital mapping is the methodology that researchers will continue to pursue into the future, especially as methods involving machine learning continue to improve results (Hengl et al., 2017). The continuous data for regions such as Northern Canada is lacking and make it difficult to produce accurate, reliable maps. However, as more research develops in Northern Canada, and as digital mapping research expands in the country, continuous data will be updated. As this continuous data is updated, the maps created here can be improved because additional variation and patterns in soil properties can be captured and used towards predicting areas where data is lacking. These are the first detailed maps of soil properties of this area of Northern Canada as such, theses maps can not only be used to assess spatial variation, magnitude, and current state in soil properties but can also be considered a starting point for future mapping in the region.

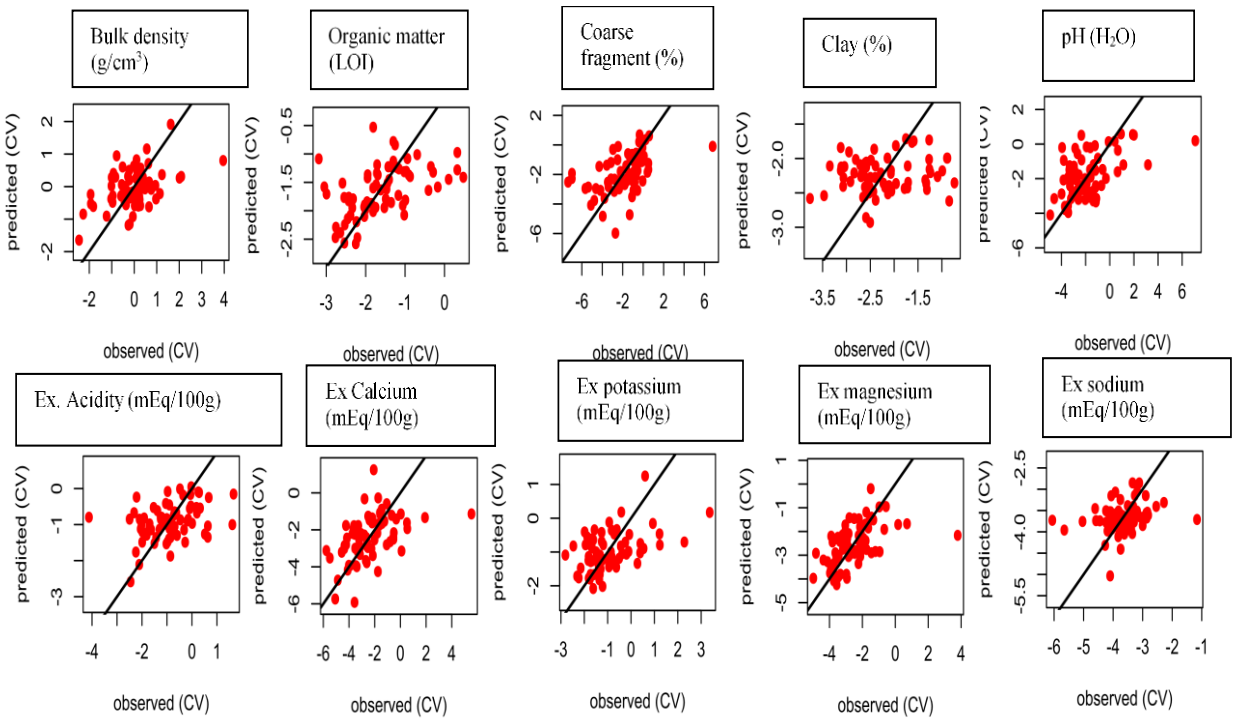

Figure 2-4 The observed versus predicted values for all transformed soil properties (bulk density, coarse fragment, organic matter [LOI], clay, exchangeable [Ex] acidity and Ex cations) for the top 50 cm of mineral soil after cross validation (CV) was performed.

Table 2-5 The variation (TVAR) described by the predictive models (%) and the normalized root mean square error (NRMSE; %) for soil properties (bulk density, coarse fragment, organic matter, clay, exchangeable [Ex] acidity and Ex cations) for the top 50 cm of mineral soil.

Units	Parameter	Variation Explained (%)	NRMSE (%)
g/cm3	Bulk density	19.8	35
%	Organic matter	26.4	37
%	Coarse fragment	21.2	132
%	Clay	0.00	61
	pH (H_2O)	24.3	194
meq/100g	Ex acidity	11.5	56
meq/100g	Ex calcium	17.7	157
meq/100g	Ex potassium	21.0	58
meq/100g	Ex magnesium	27.2	130
meq/100g	Ex sodium	2.5	63

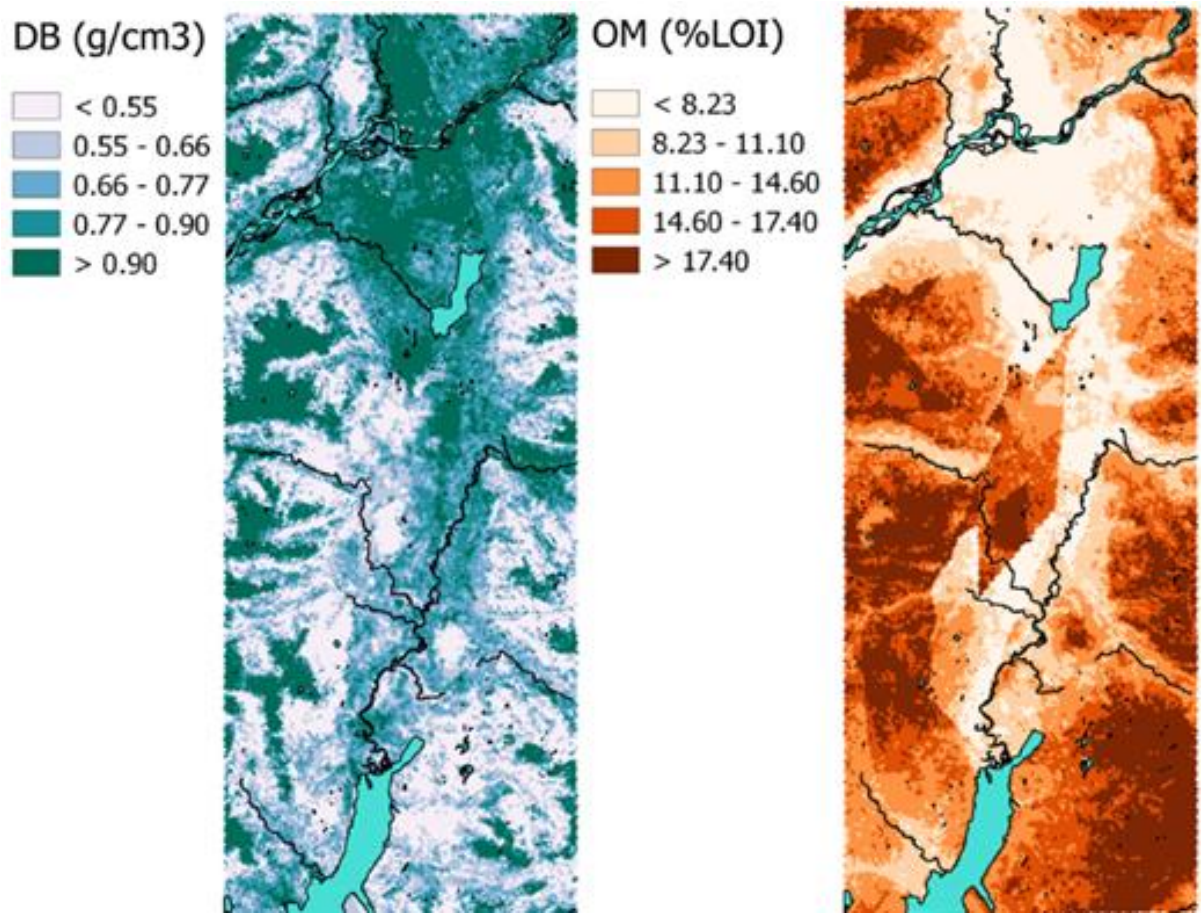

Figure 2-5 a. Predictive maps of soil properties (bulk density [Db], organic matter [OM]) for the average of the top 50 cm of mineral soil in the Kitimat Valley, British Columbia.

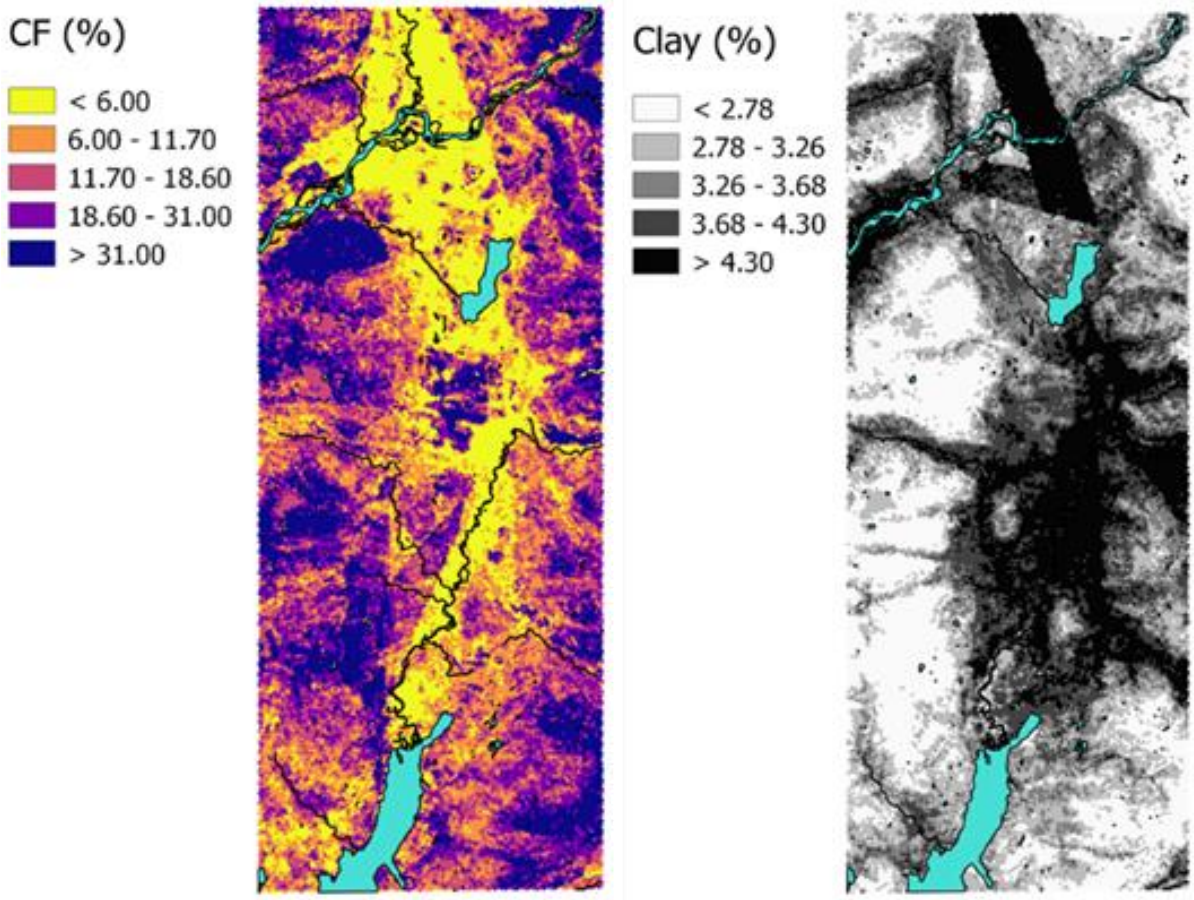

Figure 2-6 b. Predictive maps of soil properties (fragment [CF] and clay, for the average of the top 50 cm of mineral soil in the Kitimat Valley, British Columbia.

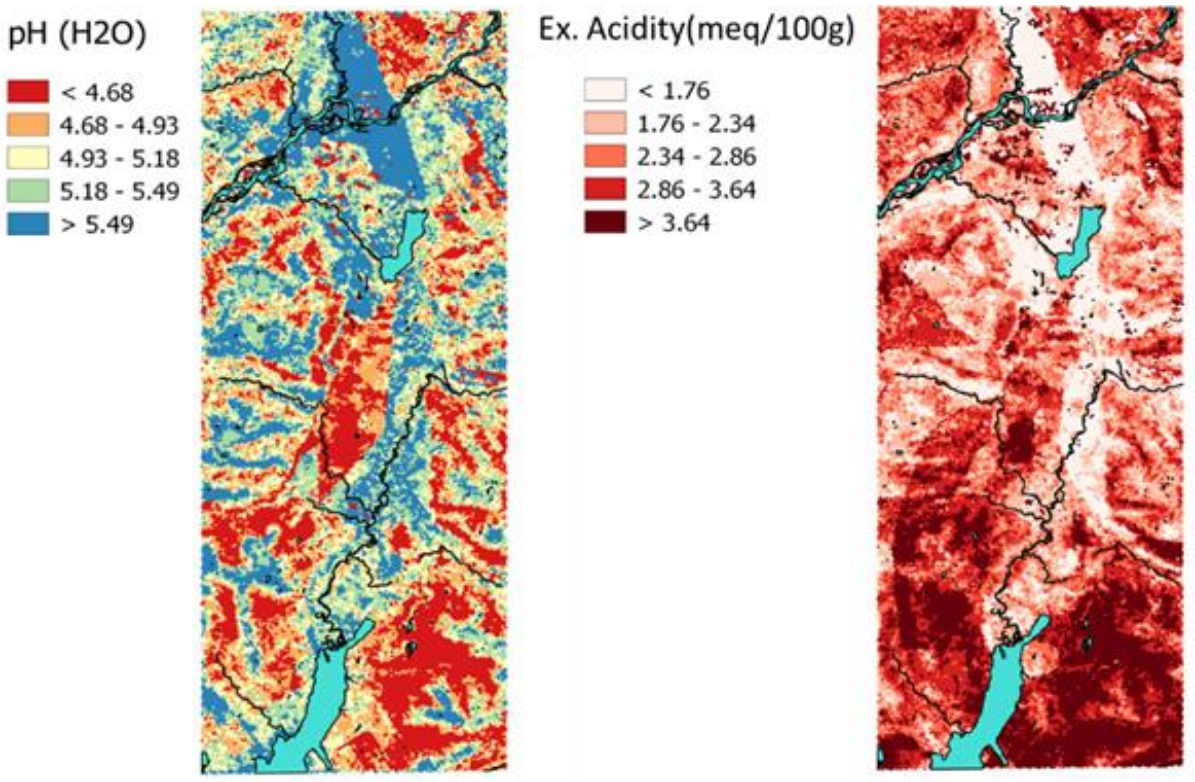

Figure 2-7 c. Predictive maps of soil properties (pH and exchangeable [Ex] acidity) for the average of the top 50 cm of mineral soil in the Kitimat Valley, British Columbia.

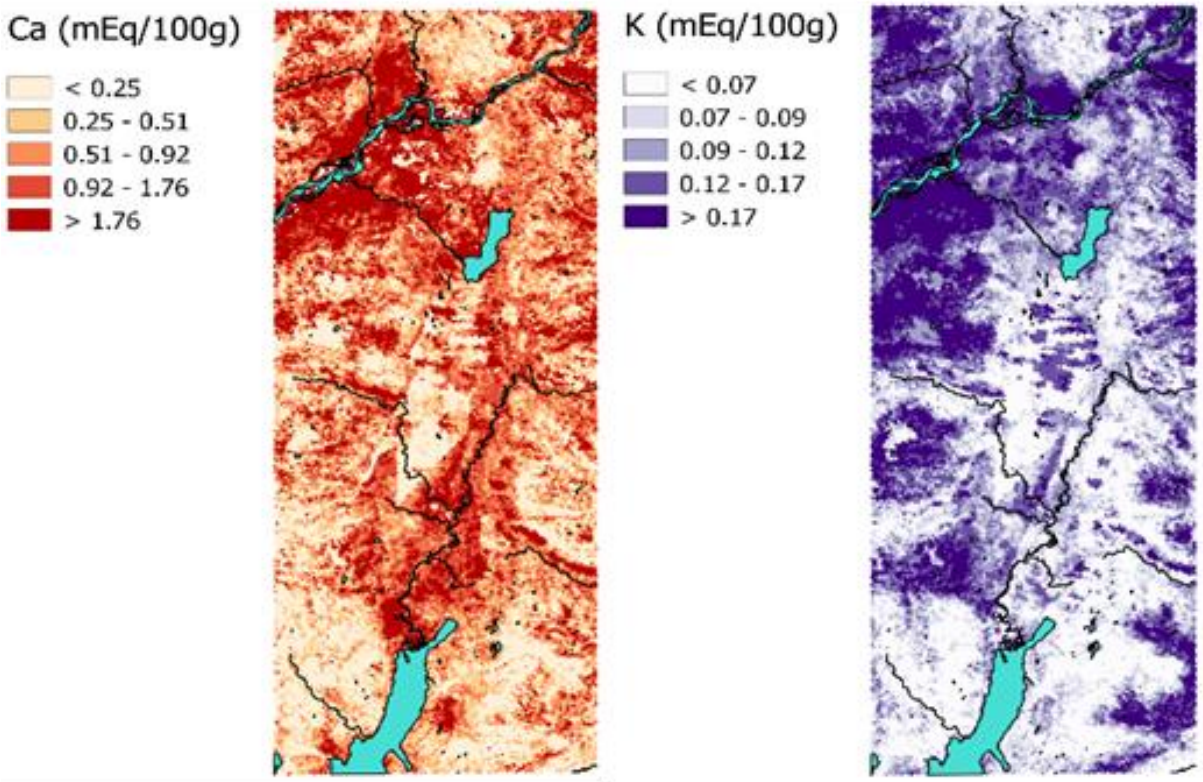

Figure 2-8 d. Predictive maps of soil properties (exchangeable [Ex] Ca^{2+} and K^{+}) for the average of the top 50 cm of mineral soil in the Kitimat Valley, British Columbia.

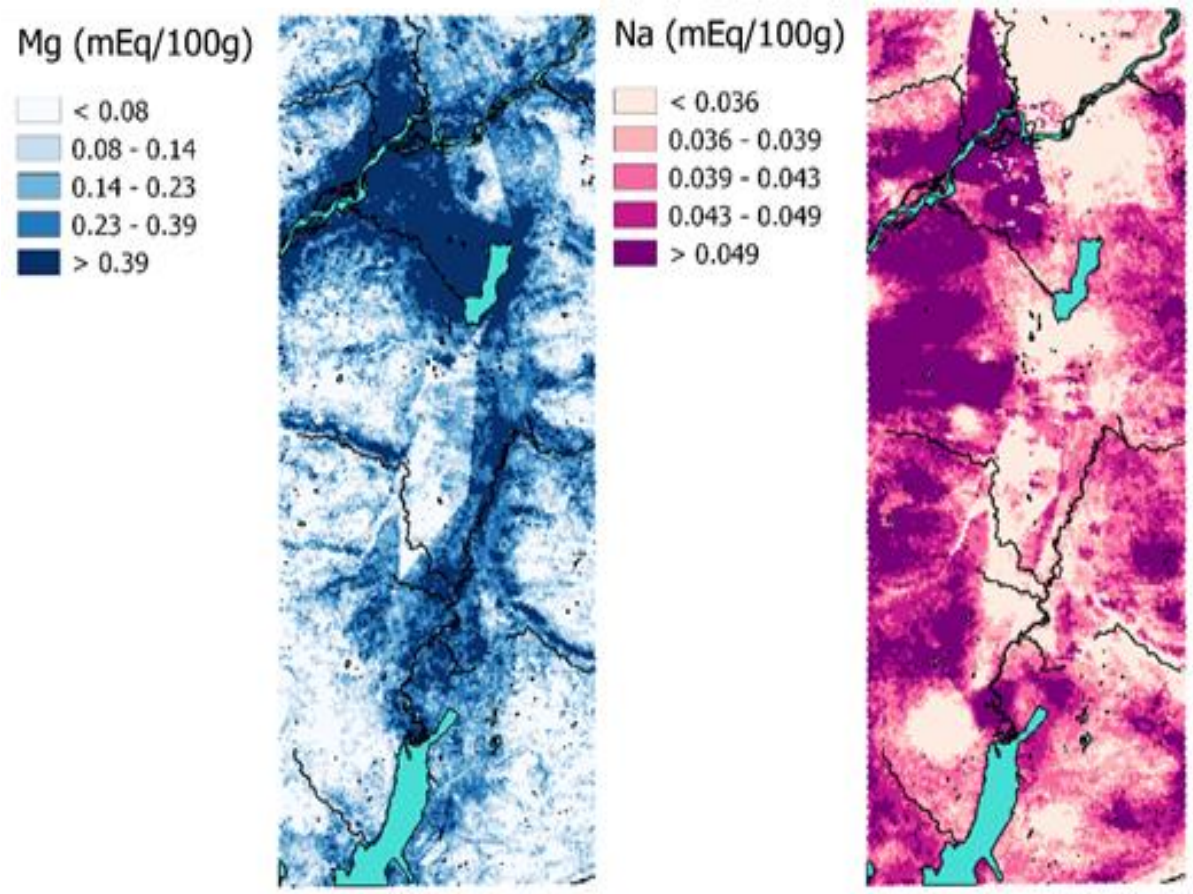

Figure 2-9 e. Predictive maps of soil properties (exchangeable [Ex] Mg^{2+} and Na^{+}) soil for the top 50 cm of mineral soil in the Kitimat Valley, British Columbia.

2.4 CONCLUSIONS

Climate and bedrock type were shown to have the highest contribution to predictive mapping. Western Hemlock, while ubiquitous in the study area, only had a small contribution. The total variation (TVAR) explained by the predictive models for the soil properties were in the range of previous studies, giving confidence in the quality of the final predictive maps. The order of confidence of the predictive maps was: Ex. Mg^{2+} > OM > pH > CF > Ex. K^{+} > Db > Ex. Ca^{2+} > Ex. acidity > Ex. Na^{+}; clay was the only soil property which was not mapped with acceptable confidence. Visually, the predictive maps showed the lower outwash plain of the valley have lower values of CF, OM, Ex. acidity, Ex. K^{+}, and Ex. Na^{+} than the mountainous upper regions. Bulk density, clay, Ex. Ca^{2+} and Mg^{2+} were found to show the opposite. Factors of uncertainty and reliability in these predictive maps were boundary alignment, completeness of the dataset (analytically and geographically), and the use of maps at different scales from different data sources.

While not all maps reached the level of confidence as previously found in the literature, there is no doubt that these soil property maps – which are the first for the region – are a helpful tool to assess the variation, state and magnitude of soil properties.

3.0 CHAPTER 3: THE PRACTICAL APPLICATION OF DIGITAL SOIL MAPPING: THE POTENTIAL IMPACTS OF AN ALUMINUM SMELTER ON SOIL ACIDIFICATION

3.1 INTRODUCTION

It is well established that atmospheric emissions from fossil fuel combustion – especially coal burning, shipping emissions, and base metal smelters, are the main sources of atmospheric sulphur (Cullis and Hirschler, 1980; Freedman and Hutchinson, 1980; Brimblecombe et al., 1989; Watson et al., 1990). Gaseous sulphur dioxide (SO_2) is the main form of atmospheric sulphur emitted from these anthropogenic sources and it is the main precursor for acidic precipitation. Once SO_2 is emitted from a point source, it can be transported within the atmosphere until it is removed via two processes; dry and wet deposition (Kellogg et al., 1972). Dry deposition occurs when SO_2 is deposited directly onto the surrounding soil and vegetation as it is heavier than air and has a short residency time (1-3 days) in the atmosphere (Garland, 1977; Schwartz, 1989). Alternatively, SO_2 can undergo oxidation reactions which ultimately results in the formation or sulphuric acid (H_2SO_4), which is deposited in rainfall (Kellogg et al., 1972; Mylona, 1996). SO_2 can be oxidized in a reaction within a singular phase such as interaction with water droplets in clouds or fog, or in a reaction, which occurs in multiple phases, such as gas to particle conversion (Bunce, 1994) Once the H_2SO_4 has been deposited onto the surrounding vegetation, water, and soil surfaces, it dissociates into H^+ and SO_4^{2-} (Guadalix and Pardo, 1991).

One of the most significant impacts of acidic deposition on soil is the leaching of base cations (Ca^{2+}, Mg^{2+}, K^+ and Na^+) and increase in concentration of aluminum (Al^{3+}) in soil solution. As the H^+ concentration in soil increases, base cations are preferentially displaced at the soil exchange sites (van Breeman et al., 1984; Reuss and Johnson, 1986; Reuss et

al., 1987; Fernandez et al., 2003). As base cations are displaced, they are then mobilized in the soil solution, and become bioavailable, so they are taken up by plants or leached from the soil by outflow of drainage water, along with SO_4^{2-}. The displacement of base cations is a neutralization process; base cations will continue to be displaced by H^+ until the base cation pools have been diminished by the acidic deposition. However, this displacement is not linear, as it is increasingly difficult to displace base cations as concentrations decrease; as such all base cations will never be totally displaced from soil (Johnson et al., 1983). Base cations are necessary for plant growth and if they are washed out of the soil, plant nutrient availability may be impacted (Likens et al., 1998; Jobaggy and Jackson, 2001). As well, when Al^{3+} is mobilized with increased H^+ concentrations, it can negatively impact vegetation as Al^{3+} is toxic to plants and has been shown to cause damage to plant tissue and effect growth (Driscoll et al., 2001; Dore et al., 2007).

How easily a soil will acidify is dependent on its buffering capacity, or simply put how much acid can be neutralized before there is a change in soil pH (Bowman et al., 2008). Buffering capacity may be indicated by certain properties such as cation exchange capacity (CEC), and base saturation. CEC is the total amount of positively charged cations (basic cations: Ca^{2+}, Mg^{2+}, K^+ and Na^+; acidic cations: H^+, Al^{3+}) present on exchange sites in soil (Sonon, 2014). Base saturation is the relative abundance of base cations on the soil exchange complex in comparison with the total cations (Sumner and Miller, 1996). Soils with higher CEC and base saturation have higher buffering capacities and are less sensitive to acidic deposition because of the higher base cation concentrations, which allows for more neutralization of H^+.

Between 1980-2010, SO_2 emissions have been reduced by 78 and 61% in the United States and Canada following the implementation of regulations to control atmospheric pollution in the Canada-US Air Quality Agreement (Canada-US AQA, 2010). However, these North American trends may not reflect the local area directly surrounding large SO_2 emission sources. As previously mentioned, the residency time of SO_2 ranges from 12 hours to 3 days (Kellogg et al., 1972; Garland, 1977; Swartz, 1989). The distance that SO_2 can travel while in the atmosphere is dependent on several meteorological conditions such as temperature, rainfall, humidity, wind speed and turbulence. Long-range transport of SO_2 is more likely under cool, dry conditions with low winds (Kellogg et al., 1972; Mylona, 1996; Khoder, 2002). Deposition has been shown to decrease exponentially with distance from point sources (Fay et al., 1985; Mylona, 1996); as such, dry deposition of S may likely have local effects close to emission sources such as aluminum smelters (Lee et al., 2011).

The Kitimat Valley is located in the northwestern coast of British Columbia (BC), Canada and is the area of interest to this study. Despite the rugged forested landscape of this northern region, there is still considerable industrial influence. The main industry of concern is the Rio Tinto BC Works aluminum smelter has emitted SO_2 as a consequence of aluminum smelting since it started production in 1954 and has been emitting SO_2 at a rate of 27 tonnes per day (t/d) since 1999 (ESSA et al., 2013). In 2015, the Kitimat Modernization Project (KMP) was completed to upgrade the smelter technology at the Rio Tinto smelting facilities. With the KMP, emissions of SO_2 were permitted to increase from 27 t/d to 42t/d. This permitted increase in SO_2 emissions will lead to an increase in sulphur deposition, and there is concern that the surrounding forest soils may be impacted (ESSA et al., 2013). Previous works have completed risk assessments on the soils in the Kitimat

Valley; the sulphur dioxide technical assessment report (STAR; ESSA et al., 2013), as well as Levasseur (2017) used the pre and post-KMP deposition scenarios (27 and 42 t/d) to estimate the exceedance of critical loads for the area. Critical load exceedances determine long-term impacts of steady state acidic deposition; however, they exclude short term buffers and give no indication of how long it will take for an area to be impacted by acidic deposition. The spatial patterns of short-term soil buffers such as cation exchange capacity (CEC), base saturation (BS), and base cation (BC) pools for the Kitimat Valley are unknown. It is important that they are evaluated as they can provide an indication of regions where effects may be observed in the near future depending of the magnitude and longevity of acidic deposition. Digital soil mapping techniques such as the ones developed for soil properties in the region can be applied here to address this knowledge gap.

The principle objective of this chapter was to apply digital soil maps of the Kitimat Valley to assess the buffering capacity and the potential impacts of increased SO_2 emissions and S deposition on the soil surrounding the Rio Tinto BC Works aluminum smelter. To do this, mineral soil samples at three fixed depths were taken from 72 locations throughout the Kitimat region during the period 2012–2016 and were analyzed for bulk density, exchangeable acidity and exchangeable cations. Then, following techniques outlined by Hengl et al. (2004), digital (predictive) soil maps were created for CEC, BS, and BC pools for the top 50 cm of mineral soil. These indicators of soil buffering capacity were used to evaluate regional sensitivity. Then, exchangeable base cation pools for the top 50 cm of mineral soil was overlaid with modelled sulphur deposition under full permitted emissions to calculate the time to base cation pool depletion. Identifying regions

with low base saturation and short time to depletion will allow for the identification of areas that are sensitive to increased acidic deposition.

3.2 METHODS

3.2.1 STUDY AREA

The Kitimat Valley is located on the northwest coast of British Columbia; its lowest point (300 m) is at the head of the Douglas Channel in Kitimat, in the south of the valley, and it extends to just past the city of Terrace, which is about 50 km to the north (ESSA, 2014; Clague, 1984). ESSA et al., 2013). The underlying terrain is comprised of mostly intrusive igneous rock, which provides an acidic, coarse, parent material (Hutchinson et al., 1979). Additionally, surficial geology mapped and described by Clague (1984) showed a significant portion of the study area, particularly the valley bottom between Kitimat and Terrace, was substantially covered by glacial deposits such as alpine complexes, till veneer, and glaciomarine sediments. These deposits can determine the sensitivity of soil, as alpine complexes and till veneers lend to the formation of podzolic soils, which are more acidic (Tamminen and Starr, 1990), and glaciomarine sediments contain greater amount of base-rich minerals and produce soils with higher base cation weathering rates (Johnson et al., 2000).

Kitimat is located predominantly within the Coastal Western Hemlock (CWH) biogeoclimatic zone, with the high elevation mountain regions being within the Alpine Tundra (AT) and Mountain Hemlock (MH) zones (Krajina, 1975). The CWH zone is on average the rainiest biogeoclimatic zone in British Columbia, with cool summers and mild winters (Meidinger and Pojar, 1991). This is true for Kitimat and Terrace, as the long-term (1981-2010) average yearly precipitation was 2774.6 and 1168.9 mm, and the annual

average temperature was 7.9 and 7.4 °C, respectively (Environment Canada, 2018).

The landcover in Kitimat Valley is dominated by dense forest, predominantly comprised of *Tsuga heteophylla* (Western Hemlock). The topography of the Kitimat Valley is very rugged, as it is flanked by mountain ranges with peaks as high as 1700 m. The principal industry in the region is the Rio Tinto BC Works smelter (ESSA et al., 2013). A liquified natural gas (LNG) project in Kitimat has been announced recently, representing added future industrial pressures on the surrounding environment. This LNG pipeline will carry natural gas to a processing facility in Kitimat where it will be condensed and shipped out of the Douglas Channel.

The Rio Tinto BC Works smelter was first built in the Kitimat Valley between 1951 and 1954, and a significant modernization project, the Kitimat Modernization Project (KMP) was completed in 2015. This modernization was designed for an increase in aluminum production by 48% from its original capacity of 280,000 tonnes per year. However, this increased production was accompanied by a permitted increased in SO_2 emissions of up to 42t/d because capturing or scrubbing the SO_2 emissions was not cost efficient. Currently, the smelter is at full production capacity, but emissions for 2016-2018 were only ~30t/d; the permitted 42t/d is required to allow for the decline of quality in green coke which may contain higher amounts of sulphur.

The current study focused on an area of 3,000 km^2 within the Kitimat Valley, surrounding the Rio Tinto BC Works smelter, spanning 30 km in the east-west direction and a 100 km in the north-south direction. This was established based on the modelling domain used by the atmospheric dispersion modelling system CALPUFF (ESSA et al., 2013). Soil samples at three fixed depths were taken from 72 locations throughout this

study domain during the period 2012–2016. The 213 individual samples from these locations were analyzed for bulk density (Db), coarse fragment (CF), organic matter (OM), pH, clay, exchangeable acidity and exchangeable base cations (Ca^{2+}, Mg^{2+}, K^{+}, and Na^{+}), which were used for predictive mapping (See Chapter 2, Figure 2-1).

3.2.2 FIELD SAMPLING AND LABORATORY METHODS

Site selection used a stratified random sampling approach to ensure spatial coverage. The strata were based on the bedrock geology map for the study region, and within each stratum a minimum of 4 sampling sites were randomly selected. Soil sampling was carried out following a common protocol; a 500 by 500 m grid was overlaid on the study domain, and sample sites were required to be accessible (the grids had to be within ~250 m from a road/trail). While sites were accessible, they were more than 50 m away from roads, rivers, and lakes, were undisturbed by human activity (no presence of forestry etc.) and had a slope of less than 45 degrees (See Chapter 2; ESSA et al., 2013). At each sampling location, a 20 m by 20 m sampling plot was established as close as possible to the centre of the 500 m by 500 m sampling grid (Chapter 2; ESSA et al., 2013). At each of the four corners and the centre of the plot, an auger was used to collect minerals soils from the fixed depths of: 0-10 cm, 15-25 cm, and 40-50 cm (below the forest floor); the five samples from each respective depth were then composited into one sample and labeled accordingly (making a total of three depth with mineral soil samples per plot). In addition, soil bulk density samples were collected from the centre of the plot using a hammer core, at the same depths as the composite soil samples. In total, 72 sites were sampled throughout the Kitimat Valley between 2012 and 2016.

Upon arrival in the laboratory, all Db samples were oven dried at 105°C for 24

hours; dried samples were then sieved in a 2mm sieve, and the coarse (>2 mm) and fine (<2 mm) materials were weighed. Composite samples were transferred into aluminum foil pans and allowed to air dry for 2 weeks; once fully dry, the composite samples were also sieved in a 2 mm sieve.

The volume of coarse fragment (CF; >2 mm), or coarse fraction displacement, was determined to calculate Db; this displacement was estimated by adding the sieved coarse fragment (> 2 mm) to 100 mL of water in a graduated cylinder and recording the volume of water that was displaced. Db was determined using the equation:

$$Db\ (g\ cm^{-3}) = \frac{Dry\ weight\ of\ fine\ (< 2\ mm) fraction\ (g)}{Soil\ core\ volume\ (cm^3) - Coarse\ fraction\ displacement\ (cm^3)}$$

Where the soil core volume was represents the inner sampling ring of the bulk density hammer.

All composite soil samples were analyzed for exchangeable cations (Ca^{2+}, K^{+}, Mg^{2+}, Na^{+}, Fe^{2+}, Mn^{2+}) using ammonium acetate (NH_4OAc), following protocols outlined by Dohrmann et al. (2012). Exchangeable acidity (H^{+} + Al^{3+}) was determined following the methods outlined by Thomas (1982) and Sims (1996). The observed soil data by depth (0-10, 15-25, 40-50 cm) was then averaged for each soil property (weighted by bulk density and depth) so the average of the top 50 cm of mineral soil was represented. Digital maps were created for this average 50 cm of mineral soil. For full details on laboratory methods and analysis see Chapter 2.

3.2.3 SULPHUR DEPOSITION

Sulphur deposition data was retrieved from the Sulphur Dioxide Technical Assessment Report (STAR; ESSA et al., 2013). The STAR technical assessment report evaluated the potential impacts of SO_2 emissions from the Rio Tinto BC Works aluminum

smelter on human health and the surrounding environment (soils, surface water, and vegetation). This assessment was based on the application to amend previous SO_2 permit, and the increase of SO_2 emissions from 27 t/d to 42 t/d to allow for higher production of aluminum. It is important to note here that SO_2 has been emitted at the pre-KMP emissions rate (27 t/d) since the 1950's, long before the permitted increase was introduced (ESSA et al., 2013). It is critical that the assessment of potential impacts must acknowledge that acidic deposition in the study area has been occurring for 65 years previous to this study. In order to determine the potential impacts of the increased post-KMP SO_2 emissions (42 t/d), STAR used the CALPUFF dispersion model to estimate wet and dry deposition throughout the study domain under post-KMP atmospheric SO_2 emissions (42 t/d). CALPUFF is a non-steady-state dispersion model which uses meteorological and geographical data to determine the plume of emissions from a point source. Based on the post-KMP emission scenario, deposition was estimated to range from ~1 to 50 kg S/ha/yr in the study area (ESSA et al., 2013; Williston et al., 2016).

3.2.4 PEDICTIVE DIGITAL SOIL MAPPING

Predictive digital soil maps were created for Db, exchangeable base cations (Ca^{2+}, Mg^{2+}, K^{+}, and Na^{+}), effective cation exchange capacity (CEC_E), and effective base saturation (BS_E) in the top 50 cm of mineral soil. Mapping was carried out using regression kriging following the generic framework outlined by Hengl et al. (2004): first, the preparation of covariate data (auxiliary variables, i.e., slope, elevation, bedrock type) was done in QGIS (2016). Secondly, the transformation of dependent variables (i.e., soil type, bedrock geology), performing regression kriging, fitting semivariograms, and back

transformation of the predictive models were completed using Statistical software packages in R (Global Soil Information Facilities (GSIF), raster, sp, rgdal, and gtools). Lastly, QGIS was used for the final visualization of the maps.

3.2.5 INDICATORS OF SOIL BUFFERING CAPACITY AND POTENTIAL IMPACTS OF INCREASED SULPHUR DEPOSITION

In this study, effective cation exchange capacity (CEC_E), effective base saturation (BS_E), and base cation (BC) pools were evaluated as indicators of soil buffering capacity and the total time to base cation depletion was calculated to evaluate the potential impacts of sulphur deposition from the aluminum smelter. This was done to assess how sensitive the soils are to acidic deposition because these measures include short term buffers of acidic deposition. They can then ultimately lend an understanding of the temporal influence of acidic deposition and determine not only if an ecosystem is affected but also when it is likely the impacts will be seen. As discussed in Chapter 2, this is unlike how typical risk assessments are completed, where critical loads of atmospheric nitrogen and sulphur are used as indicators of ecosystem sensitivity to acidification following the LRTAP Convention (Chapter 2; UNECE, 2015). However, while critical loads are widely used in risk assessment, they produce long-term steady-state estimates; this means that they do not include short-term buffering processes such as buffering via exchangeable base cations (Spranger et al, 2008). As such, CEC_E, BS_E, and BC pools were used to assess the short-term buffering capacity of the soil and potential impacts of acidic deposition from the aluminum smelter.

Cation exchange capacity (CEC) is a measure of the soil's ability to hold positively charged ions. As such, it influences soil structure stability, nutrient availability, and provides a buffer against soil acidification (Sumner and Miller, 1996). CEC is typically

measured by one extraction processes using NH_4Cl (Nissinen and Ilvesniemi, 1990). When NH_4Cl is added to a soil sample, all soil exchange sites are saturated with ammonia; the amount of ammonia is then measured and the total positive charge a soil can hold is determined (Hendershot et el., 1993; Tucker, 1985). Alternatively, if individual exchangeable cations are extracted separately through exchangeable base cation and exchangeable acidity extractions, and summed together, the effective CEC (CEC_E) is estimated. CEC_E was estimated as the sum of exchangeable Ca^{2+}, K^+, Mg^{2+}, Na^+, Al^{3+} and H^+ concentrations (Tamminen and Starr, 1990).

Effective base saturation is the percentage of the CEC_E which is made up of the base cations Ca^{2+}, K^+, Mg^{2+}, and Na^+. Base saturation is an indicator of a soils ability to buffer acidic deposition (Shoenholtz et al., 2000). The BS_E (%) was calculated by dividing the sum of Ca^{2+}, K^+, Mg^{2+}, and Na^+ by the CEC_E and then multiplied by 100. In this study, values of 10 and 20% were recommended limits of BS_E. These values were chosen because previously it has been recommended that soils do not fall below ~20% BS_E in order maintain soil quality and to protect tree health and forest ecosystem functions (Ouimet et al., 2006). Additionally, it has been shown that if the BS_E of a soil reaches 10%, deleterious impacts on the soil can occur, such as soil acidification and soil toxicity due to increased Al^{3+} concentrations. So, for the observed and mapped data, the percentage of sites or area, respectively, that had a BS_E below 10 and 20% were determined. This was done using a cumulative frequency plot for the observed data, and zonal raster statistics – which calculated the area of BS_E – using QGIS for the predictive maps.

The base cation pool, which is the total amount of base cations available in the soil (at the point risk of assessment), and like base saturation, it is an indicator of a soils ability

to buffer acidic deposition. i.e., a larger base cation pool can buffer a greater magnitude of acidity. Base cation pools (meq/m^2) were calculated using the following equation:

$$BC\ pool\ (\frac{meq}{m^2}) = \frac{(Conc.of\ base\ cation\ (meq/100g)}{100} X\ Db\left(\frac{g}{cm^3}\right) X\ 100000\ X\ Depth\ (50\ cm)$$

The time to base cation depletion is the amount of time (in years) it will theoretically take continued acidic deposition to deplete the entire base cation pool. The time to depletion for the top 50 cm of mineral soil was calculated as the base cation pool (meq/m^2) divided by estimated wet and dry sulphur deposition (meq/m^2/yr) under the post-KMP atmospheric SO_2 emission scenario (42 t/d) (ESSA et al., 2013). Deposition estimates were retrieved in kg S/ha/yr and converted from kg S/ha/yr to meq/m2/year. It is important to note that time to depletion is the worst-case scenario and should be viewed as such. The scenario calculated in this study is based on permitted SO_2 emissions (42t/d); this emissions scenario has not yet been reached, as averages for 2016-2018 were ~30t/d, and therefore currently S deposition is not as high as what was used in to calculate time to depletion. Additionally, only total BC pools were used to estimate time of depletion; the calculation did not take into account other sources of base cations into the soil system, such as the BC pool found in the organic horizon of soil, base cation weathering, and base cation deposition (Rosenstock et al; 2019).

3.3 RESULTS AND DISCUSSSION

3.3.1 QUANTITATIVE DATA

Within the top 50 cm of mineral soil, the average CEC_E and BS_E across the 72 sampling sites were 5.0 meq/100g (1.1-15.4 meq/100g) and 39.2% (6.4-98.8%). The variation of CEC_E and BS_E were low, with a CV of 59% and 66%, respectively (Table 3-1). Approximately 7% and 30% of sample sites (n = 72) had a BS_E < 10 and 20% respectively (Figure 3-1).

CEC_E for the 0-50 cm depth was half of what has been found in 19 forest soils across the Georgia Basin, British Columbia (10.3 meq/100g) at the 0-100 cm depth (Mongeon et al 2010). The range in values seen in this study were similar to a previous study of the Catskills Mountainous southeastern New York State, which is a relatively pristine area of the state; here this study found 2.0-17.4 meq/100g for the 0-50 cm depth in 51 hardwood forest soil samples (Johnson et al., 2000). BS_E values for this study were also comparable to previous studies completed in Finland; the first of which found BS_E of 27 and 35% for the 5-20 cm and 20-40 cm depths for 65 sample locations (Tamminen and Starr, 1990). The second study found a BS_E value of 40.9% for the 50-60 cm depth across 320 sample locations (Nuotio et al., 1990).

The BC pool for the top 50 cm of mineral soil had an average of 8369 meq/m^2 (520-67244 meq/m^2), with almost three times the variation than CEC_E and BS_E with a CV of 144% (Table 3-1). The dominant exchangeable cation in the 0-50 cm depth was calcium, which contributed to 73% of the total pool, which is similar to previous studies (Tamminen and Starr, 1990; Nuotio et al., 1990; Joslin et al., 1992; Johnson et al., 2000).

Table 3-1 Minimum, maximum, average, coefficient of variation (CV; %) of the observed soil data for the soil properties: CECE (meq/100g), BSE (%), Cation pools (Ca, K, Mg, Na, and BC; meq/m2) for the top 50 cm of mineral soil.

Parameter	Units	Min	Max	Average	CV (%)
CEC_E	(meq/100g)	1.1	15.4	5.0	59
BS_E	%	6.4	98.8	39.2	66
Ca pool	(meq/m^2)	153.8	56194.8	6134.2	152
K pool	(meq/m^2)	67.0	2061.3	415.9	90
Mg pool	(meq/m^2)	72.4	15872.6	1511.7	173
Na pool	(meq/m^2)	11.7	7673.1	307.3	296
BC pool	(meq/m^2)	520.5	67243.9	8369.1	144

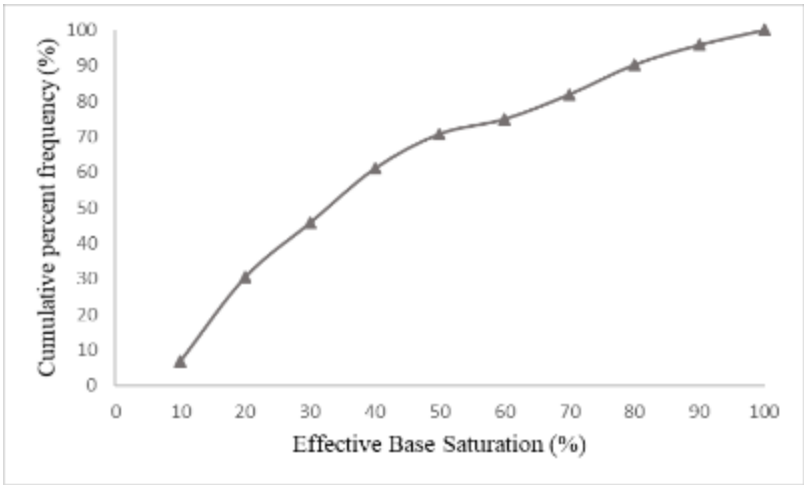

Figure 3-1 Cumulative frequency plot for the effective base saturation (%) in the top 50 cm of mineral soil.

3.3.2 DIGITAL MAPS AND REGIONAL SOIL BUFFERING CAPACITY

Average CEC_E in the top 50 cm of mineral soil across the mapped study domain was 4.23 meq/100g; the range was 0.75-20.77 meq/100g, with a CV of 38%. Average BS_E was 33.2%, with a range of 1.7-99.9%, and a CV of 66% (Table 3-2). The variations for the mapped CEC_E was much lower than the observed data, the variations for the observed and mapped BS_E were the same (Table 3-1, Table 3-2). Also note that while the high end of the range for BS_E reached ~100%, only 0.14% of the total area had a BS_E of 99%. Lastly, within the top 50 cm of mineral soil, 16.7% and 37.8% of the total mapped study area had a BS_E of less than 10 and 20%; this would indicate that a substantial percentage of the study area was within the limits of BS_E set for this study.

The BC pool had an average of 5725 meq/m^2, with a range of 210-78627 meq/m^2, and a CV of 112% (Table 3-2). This average was lower than the average for the observed weighted soil data (observed was 8369 meq/m^2), which showed a greater range in values (Table 3-1, Table 3-2). As was seen in the observed data, the variation for the BC pool was much higher than the variation seen in the CEC_E and BS_E maps (Table 3-1, Table 3-2).

Additionally, calcium was also the dominating cation for the 0-50 depth, comprising 70% of the total pool. It was also interesting that for the mapped K pool, the variation was lower in the map values than what was seen in the observed data, even though there was a higher range in the map data (Table 3-1, Table 3-2).

The glacial outwash plain generally had lower predicted CEC_E than the mountainous areas; particularly, the mountainous areas to the north-west and south-east had the highest CEC_E (Figure 3-2). This spatial pattern was also seen in the digital maps for BS_E and BC pools. The glacial outwash plain had higher BS_E values and higher BC pools than the mountainous areas; it also appeared that a considerable proportion of the southern region of the study area had a BS_E of 10% and lower BC pools (Figure 3-2). These areas, as previously mentioned, are important to note, as areas of lower BS_E values may indicate areas which are more sensitive to acidic deposition. The higher values in the glacial outwash plain are likely due to the surficial material of the area; glaciofluvial deposits may have higher base rich minerals (Egli et al., 2001), and so these areas would have higher base cation pools.

It should also be noted that a rough diamond shape was seen in many of the maps, particularly the maps for CEC_E and BC pools (Figure 3-2). Variables which have stronger influences on the dependent variable can cause a distinct spatial pattern such as the diamond shape seen in the maps of CEC_E and BC pools. When comparing the size and shape of the Quartz Dioritic (QD) bedrock map to this distinct shape, it was determined to be the same. Quartz dioritic bedrock was one of many geology maps which are part of a province-wide repository maintained by the British Columbia Geological Survey (Miller et al., 2017). It was also one of the most dominant bedrock types in the study area, covering

almost 30% (ESSA et al., 2013). From this, it can be determined that there was a strong relationship between areas underlain with QD bedrock and higher BC concentrations. This may have been seen based on the weathering products of QD; once weathered, QD forms saprolite, a porous and thoroughly decomposed rock, containing quartz and kaolinite (Turner et al., 2003). In BC, these saprolites are formed on glacial tills in rolling terrain, much like that of Kitimat (De Kimpe et al, 1984). While quartz is hard and often slow to weather, kaolinite is an important weathering product because it is a type of silicate clay that contributes negative charges where exchangeable base cations adhere to (Brady, 1984). Thus, the strong relationship between QD and higher base cation concentrations.

Table 3-2 Minimum, maximum, average, coefficient of variation (CV; %) of the predictive maps created for the soil properties: CECE (meq/100g), BSE (%), Cation pools (Ca, K, Mg, Na, and BC; meq/m2) at the 0-50 cm soil depth.

Parameter	Units	Min	Max	Average	CV (%)
CEC_E	meq/100g	0.8	20.8	4.3	38
BS_E	%	1.7	99.9	33.2	66
Ca pool	meq/m^2	0.00	66184.0	4006.0	132
K pool	meq/m^2	43.1	2999.07	451.2	79
Mg pool	meq/m^2	33.6	26241.9	1110.4	198
Na pool	meq/m^2	36.8	1603.4	157.8	46
BC pool	meq/m^2	210.4	78627.0	5725.3	112

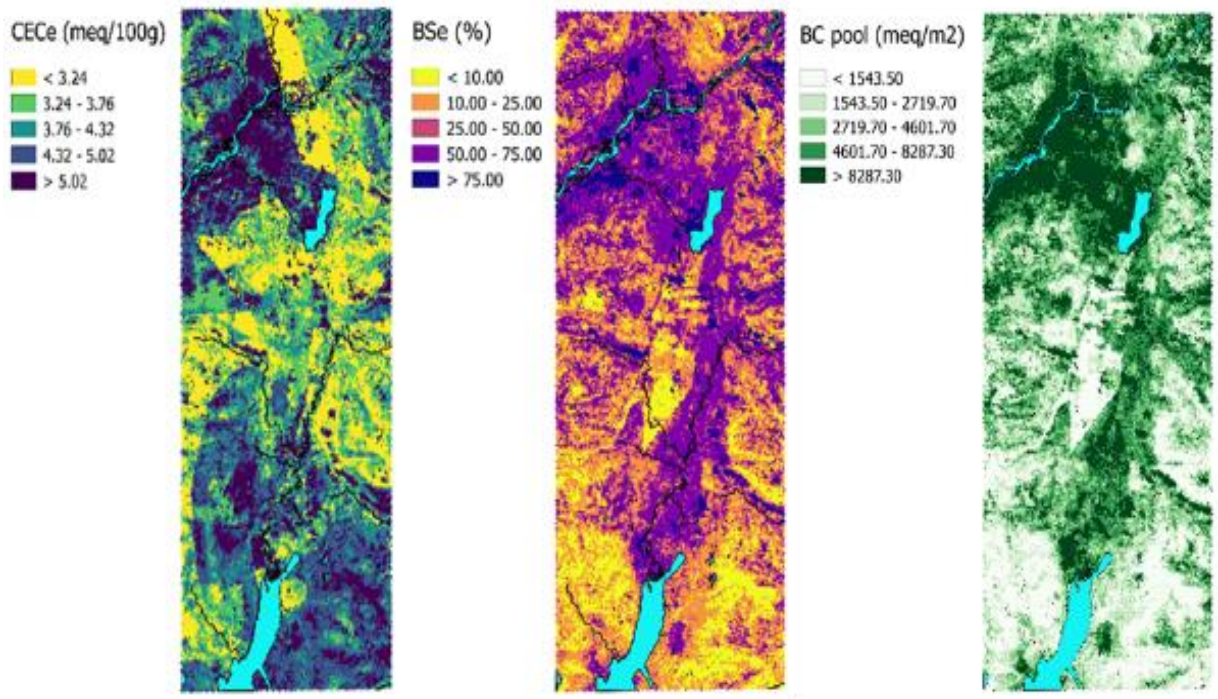

Figure 3-2 Digital soil maps of CECE (meq/100g), BSE (%), and base cation (BC) pool (meq/m2) for the 0-50 cm soil depth in the Kitimat Valley, British Columbia.

3.3.3 POTENTIAL IMPACTS OF SULPHUR DEPOSITION

Average S deposition across the study domain was 19.3 meq/m^2/yr, with a range of 0.4-814.3 meq/m^2/yr and a CV of 78.1%. Deposition rates greater than 800 meq/m^2/yr were found closest to the smelter, located in the southwest corner of the study domain (Figure 3-3). As distance from the smelter increased, deposition decreased, with the outer boundaries of the study domain receiving <5 meq/m^2/yr (Figure 3-3). This was to be expected based on the effect of rainfall and wind direction on S deposition. Increased rainfall may affect the distance in which emitted SO_2 travels in the atmosphere in two ways; first, increased rainfall could increase the homogenous oxidation reaction which occurs to create the H_2SO_4, and secondly, rainfall may intercept sulfate particulate in the air, removing them in a process called rainout (Kellogg et al., 1972). As well, the surrounding

Hazleton and Coastal mountains create a corridor for the valley, preventing other possible wind. Therefore, wind direction could have also been determined to be a factor in S deposition because of the predominant south-north winds in the Kitimat Valley which control the movement of the plume from the smelter. Ultimately, this would mean that emitted SO_2 would be dominated by wet deposition processes that determine short-range rather than long-range transport. As previously mentioned, the valley is located in one of the rainiest bioegeoclimatic zones in British Columbia, receiving up to 2775 mm of rain on average annually (Meidinger and Pojar, 1991; Environment Canada, 2018), and so the amount of precipitation the valley received may have affected the deposition pattern.

The average time to depletion for the base cation pool in the top 50 cm of mineral soil under modelled S deposition (42 t/d) was 773 years, with a range of 2.6-29741 years and a CV of 181 %. Approximately 8% of the soils mapped in the study area had a depletion time of 50 years or less. Depletion times were shortest (less than 50 years) along the glacial outwash plains and longest along the mountainous areas with depletions times greater than 750 years. This time to depletion pattern closely follows the pattern of the S deposition plume (Figure 3-4), with the majority of the areas with the lowest time to depletion under the highest deposition values (Figure 3-3, Figure 3-4). As depletion times closely followed the pattern of the S deposition plume, it may be suggestive that time-to-depletion was driven by high modelled deposition. However, not all areas with short time to depletion were found under the areas of elevated deposition, such as the southeastern corner of the study area, and the northern valley bottom (Figure 3-4). This was because these areas had small BC pools which were not large enough to buffer the amount of acidic deposition they received (Figure 3-2). It is likely that soil type played a role in the small BC pool; one of

the most dominant soil types in the study area was podzol soil, which are acidic in a nature and contain low concentrations of base cations (Peterson, 1980).

It is also important to acknowledge that uncertainty in digital mapping is prevalent and may have impacted the variation and quality of the final maps. As discussed in Chapter 2, there were many sources of uncertainty in digital maps which have been identified by Finke (2006). The first that applies to the maps created in this chapter is completeness of the dataset (both in analysis and in terms of spatial coverage of the study domain); in this study, it may be that the south-western corner had less samples than the rest of the study area, and therefore there would have been greater uncertainty in the predictions in that area, potentially skewing the predictions. Also, there were three sites in which singular depths which were missing and not analyzed, so analysis was not entirely complete for all depths at all 72 sites. As well, how up to date the data is and errors that may occur when maps of different scales and sources are combined may be sources of uncertainty in continuous soil data and digital maps. Specifically, the issue of combining maps from different sources was discussed as a source of uncertainty in the soil type covariate map used to create the predictive maps (Omuto et al., 2012; Grunwald et al, 2011). Additionally, as these sources of uncertainty affected the digital maps previously produced for soil properties (Chapter 2) they may have been further compounded here when they were used to calculate the maps in this chapter. This is because there is a combined uncertainty from many sources used to produce the final maps: the raster maps for base cation concentrations and bulk density were used to calculate the total BC pool, as well as uncertainty in the S deposition data. It has been

acknowledged that S deposition was overestimated previously; as such, the estimates of time to base cation depletion cannot be seen as conservative and should be revisited.

While estimates of time to depletion suggest that 8% (~240 km^2) of the forest soils in the study region will lose their exchangeable base cations (due to the acidic buffering of nutrient pools) in less than 50 years, this represents the worst-case scenario. For context, the smelter has been producing emissions of SO_2 for more than 50 years at the rate of 27 t/d (ESSA et al., 2013); it is possible that the acidic deposition from the last 65 years has already depleted the soils. It is also paramount that it is understood that base cation pools will never be fully depleted; as base cation concentrations in the soil decrease, displacement becomes increasing difficult, meaning there will always be some concentration of base cations in the soil (Johnson et al., 1983). These maps are a worst-case, simplified analysis and do not represent the entirety of what is occurring in the soil. This is because only one source of base cations (the base cation pool) was considered; two of the largest sources of base cations into terrestrial systems which were not considered are atmospheric deposition and mineral weathering. Atmospheric deposition of base cations occurs through both natural and anthropogenic processes such as dust deposition, fossil fuel combustion and agricultural practices (Hedin et al., 1994; Lovblad et al., 2004). Mineral weathering occurs when the parent material of the soil is broken down over time and base cations are released (Ouimet et al., 2005). Weathering rates for the Kitimat Valley have been previously estimated; most of the study area had weathering rates between 50-150 meq/m^2/year, with areas south of the Kitimat Village and high elevation areas to the south-west of Terrace having the lowest weather rates of 25-50 meq/m^2/year (ESSA et al., 2013). It was also found that on average, base cation deposition was about 6 meq/m^2/year

for the Kitimat Valley (KAEEA, 2014). It is seen in the deposition map that only a very small area of the study region had very high deposition (Figure 3-3). As such, there were areas (i.e., North of the Douglas Channel) in the study region where the range in time to depletion were shorter, showing a decreased range of ability to buffer the acidic deposition (Figure 3-4). Again, it is unrealistic to assume that these areas will be depleted in 50 years or less, as only base cation pools, which affect the short-term buffing of acid, were evaluated. Other sources and fluxes into the system were not included.

Lastly, it is important to address that this type of assessment is looking at a static point in time, while soil properties and S deposition models are dynamic. Soil data was collected once for each site, so it represents one point in one moment of time between 2012-2015, and average S deposition data for a year was used. As the smelter has been operating for the last 65 years, it is very unlikely that temporal changes in soil as well as fluxes of inputs of base cations and changes in deposition throughout time were captured with this point data. As a result, this is another reason that findings here should be considered a first attempt at assessing impacts through predictive mapping rather than definitive findings.

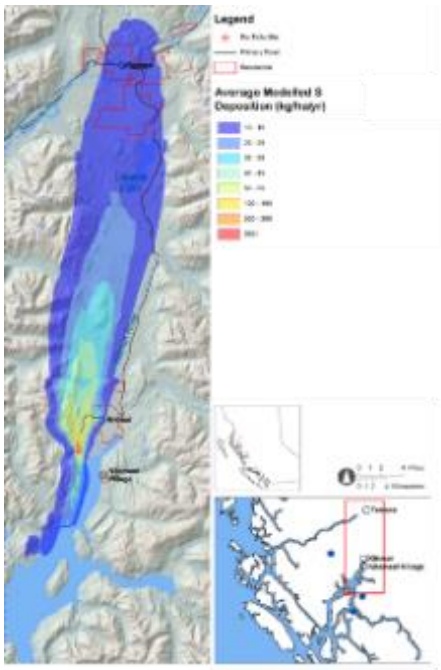

Figure 3-3 Modelled Sulphur deposition (kg SO_4^{2-} /ha/yr) for the Kitimat Valley, British Columbia under the post-KMP permitted emissions scenario of 42 t/d.

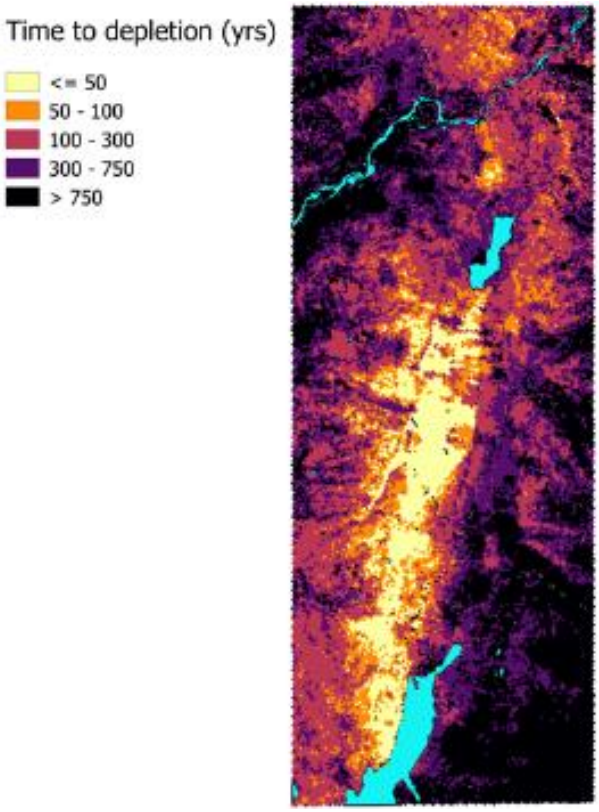

Figure 3-4 Time to depletion map (years) for the top 50 cm of mineral soil in the Kitimat Valley, British Columbia.

3.4 CONCLUSIONS

The digital map of BS_E for the top 50 cm of mineral soil showed that 16.7% (~500 km^2) and 37.8% (~1,100 km^2) of the mapped soil area had a BS_E of less than 10 and 20%. This indicated that a substantial percentage of the study area is within the BS_E limits set for this study, and areas within or below these limits may show impacts to ecosystem function, as well as increased Al^{3+} concentrations which is toxic to vegetation and could lead to a decline in tree health. The BC pools were highly variable, the southern region of the study area had lower pools than those of the glacial outwash plain; glaciofluvial sediments contributed to the larger base cation pools.

Less than 10% of the study area (~240 km^2) had a depletion time of 50 years or less, with depletion times closely following the pattern of the S deposition plume, suggesting time-to-depletion was driven by high modelled deposition. However, small areas in southeastern corner of the study area, and the northern valley bottom showed time to depletions in the 50-100-year range, which may indicative of low small BC pools. Time to depletion estimates were calculated as a worst-case scenario, where sources of base cations such as atmospheric deposition and mineral weathering, as well as sinks and removals, were not considered. If considered, average base cation deposition for the area (6 meq/m^2/yr) and average base cation weathering rates for the study area (50-100 meq/m^2/yr) would increase the time in which base cation pools are depleted by S deposition in some areas. However, there are areas in which the highest deposition rate is still greater than base cation pools, deposition, and weathering combined. These areas identified as having the lowest base cation weathering rates were found south of the Kitimat Village and the high elevation areas to the south-west of Terrace. It was identified that these were the areas which could potentially be impacted by the increased SO_2 emissions.

4.0 FINAL CONCLUSIONS

General conclusions

In the first manuscript, it was seen that in the observed soil data, CF, clay, and pH all showed a decrease in the coefficient of variation with an increase in depth. Variation within the soil depths could be explained through soil processes such as nutrient cycling and biological processes which occur at soil surface and decrease with depth. The range in elevation (10-1287 m), slope of the rugged terrain, as well as the dominant parent material (quartz diorite (QD)) in the study area may have resulted in the range of variation found in the soil properties for the average top 50 cm of soil. Bulk density was found to have the lowest variation of 38.5%, while Ex. Na^+ had the highest, with 261.1%.

When the predictive maps of the average top 50 cm of soil were evaluated, it was found that total variation (TVAR) explained by the predictive model for the soil properties were similar to those of the literature, giving confidence in the quality of the final predictive maps. The exception to this was clay, which was not mapped with acceptable confidence. The order of confidence of the predictive maps was: Ex. Mg^{2+} > OM > pH > CF > Ex. K^+ > Db > Ex. Ca^{2+} > Ex. acidity > Ex. Na^+. Ultimately, the maps produced here are the first of their kind for the Kitimat Valley, and are an invaluable tool in which the state, magnitude and variation of the soil properties can be assessed

These predictive maps were then used to predict indicators of soil buffering capacity (effective cation exchange capacity (CEC_E), effective base saturation (BS_E), and base cation (BC) pools), as well as assess the potential impact of increased SO_2 emissions on the surrounding forest soil.

In the second manuscript, the digital map of BS_E for the top 50 cm of mineral soil showed that 16.7% (~500 km^2) and 37.8% (~1,100 km^2) of the total area had a BS_E of less

than 10 and 20%. This indicated that a large portion of the study area is within the BS_E limits set for this study. The BC pool was also quite variable, and maps showed that the southern region of the study area had lower pools than those of the glacial outwash plain; glaciofluvial sediments were found to contribute to the larger base cation pools. A rough diamond shape was seen in many of the maps, particularly the maps for CEC_E and BC pools. This was found to be the result of a strong relationship between QD bedrock and higher concentrations of base cations. QD was one of the most dominant bedrock types in the study area; it is possible this relationship was seen due to the weathering products of QD, which includes kaolinite, a type of silicate clay which has higher exchange sites for cations to adhere to.

Average total sulphur (S) deposition across the study domain showed that deposition was highest under the plume. This suggested that time-to-depletion was driven by high modelled deposition. Less than 10% of the study area (~240 km^2) had a depletion time of 50 years or less; depletion times were shortest along the glacial outwash plains and longest along the mountainous areas. This time to depletion pattern closely follows the pattern of the S deposition plume. However, the southeastern corner of the study area, and the northern valley bottom had short depletion times under low S deposition; this was a result of small BC pools in those areas. It is important to note that these areas may have a shorter temporal range of buffering acidic deposition and should be monitored.

Time to depletion estimates were calculated as a worst-case scenario, where sources of base cations such as atmospheric deposition and mineral weathering, were not considered. The smelter has been producing SO_2 for the last 65 years and soils have not yet been depleted of their BC pools. Additionally, this study has observed a snapshot of

those years based on data for one year. It was difficult to determine whether those dynamic processes of soils and their interaction with acidic deposition was captured by this data and whether sensitive areas seen were already sensitive from the first 60 years previous to this work.

Study significance and limitations

As previously mentioned, more soil surveys have been done in recent years because of increased industrialization the Kitimat Valley including the KMP and LNG pipeline. These surveys have produced soil data, and the LNG data was used to create simple maps of soil classes. Additionally, a map of weathering rates using simple digital mapping techniques has been made. While all this work has been done, the soil properties discussed throughout this thesis have never been mapped for the Kitimat Valley. This study was the first to apply the regression kriging (RK) approach to mapping soil properties in the Kitimat Valley. This is important because data availability across Canada, especially in remote northern areas such as Kitimat can be scarce, and so these maps can now contribute to the data as well as illustrate the variation, state and magnitude of soil properties there. Lastly, areas in the Kitimat Valley which could be potentially impacted by the increased acidic deposition were identified. It was seen in the second manuscript that predictive digital mapping can be applied to large, real-world environmental problems, making risk assessments at these large scales easier to approach. This is a contribution to the predictive mapping field in Canada, because it was a showcase in how RK was used to improve regional soil information to support the assessment of environmental impacts of industrial emissions.

The main limitations of this study were data availability and uncertainty. Availability is a limitation as high resolution maps of bedrock geology and soil class can be hard to access for remote areas such as Kitimat. This is especially true for forest soils, which have been under-sampled as a result of a historic focus of soil mapping in Canada on agricultural areas to improve and maintain the industry.

As was discussed in both chapters of this thesis, there were many sources of uncertainty identified which affect digital mapping. Completeness of analysis and spatial coverage of the study domain was the first source identified. Three sites in this study had singular depths which were missing and not analyzed, so analysis was not entirely complete for all depths at all 72 sites. As well, the south-western corner had less samples than the rest of the study area, and therefore greater uncertainty in the predictions, potentially causing a skew in the over-all predictions. As well, errors that occur when maps of different scales and sources are combined may be sources of uncertainty in continuous soil data and digital maps. Specifically, this example of uncertainty arose in the covariate map of soil type. Additionally, the sources of uncertainty which affected the digital maps of soil properties may have been further compounded when they were used to calculate the maps for CEC_E, BS_E, and BC pools. This is because there is a combined uncertainty from many sources used to produce the final maps: the raster maps for base cation concentrations and bulk density were used to calculate the total BC pool. Lastly, uncertainty in the S deposition data has been identified; it has been acknowledged that S deposition was previously overestimated; as such, time to depletion was likely overestimated and times are longer in actuality.

Recommendations

Future work using predictive mapping in the Kitimat Valley should investigate continued soil sampling in the south-west corner of the study area. Additional samples would mean that a training data set could be set aside to better train and validate the model. As well, as continuous maps are updated through sampling initiatives and mapping research, the predictive maps created from them will also improve, so it is important that these updates continue. This study provided an initial application of RK and should be built upon and used in forested regions in Canada. Lastly, it is suggested that RK mapping techniques be applied to the weathering rates, bedrock geology and soil class maps which have already been created for the Kitimat Valley. These maps exist to some extent in this area but could be updated and improved; traditional mapping techniques were used to create them, which do not provide the continuous coverage that RK provides. Having a continuous map may provide more detail as it gives data for 250 m by 250 m grids rather than large polygons of one data type. This detail may further contribute to the understanding of weathering rates, bedrock geology and soil class.

5.0 WORKS CITED

Anderson, D. W. 1988. The effect of parent material and soil development on nutrient cycling in temperate ecosystems. Biogeochemistry, 5, 71-97.

Andrews, J. A., and Schlesinger, W. H. 2001. Soil CO_2 dynamics, acidification, and chemical weathering in a temperate forest with experimental CO_2 enrichment. Global Biogeochemical Cycles, 15, 149-162.

Aune, J. B., and Lal, R. 1995. The tropical soil productivity calculator—a model for assessing effects of soil management on productivity. Soil management: Experimental basis for sustainability and environmental quality, 499-520.

Babish, G. 2006. Geostatistics without tears: A practical guide to geostatistics, Variograms and Kriging. Environment Canada Ecological Research Division, Regina, Saskatchewan, Canada.

Baldwin, M., Kellogg, C. E., and Thorp, J. 1938. Soil classification. pp. 979-1001. Indianapolis: Bobbs-Merrill.

Baver, L. D. 1934. A classification of soil structure and its relation to the main soil groups. Soil Science Society of America Journal, 15, 107-109.

Bishop, T. F. A., and McBratney, A. B. 2001. A comparison of prediction methods for the creation of field-extent soil property maps. Geoderma, 103. 149-160.

Blöchliger, G. 1931. Mikrobiologische Untersuchungen an verwitternden Schrattenkalkfelsen Doctoral dissertation, ETH Zurich.

Bowman, W. D., Cleveland, C. C., Halada, L., Hresko, J., and Baron, J. S. 2008. Negative impact of nitrogen deposition on soil buffering capacity. Nature Geoscience. 11, 767.

Brady, N. C., Weil, R. R., and Brady, N. C. 2010. Elements of the nature and properties of soils No. 631.4 B733E. Upper Saddle River, NJ: Pearson educational international.

Brady, N. C. 1984. The nature and properties of soils (Vol. 11). New York, NY: Macmillan Publishing Company.

Braun-Blanquet, J., Jenny, H. 1926. Vegetations-Entwicklung und Bodenbildung in der alpinen Stufe der Zentralalpen Klimaxgebiet des Caricion curvulae: mit besonderer Berücksichtigung der Verhältnisse im schweizerischen Nationalparkgebiet; mit 36 Tabellen. Fretz.

Brimblecombe, P., Hammer, C., Rodhe, H., Ryaboshapko, A., and Boutron, C. F. 1989. Human influence on the sulphur cycle. Evolution of the global biogeochemical sulphur cycle, 77-121.

Bunce, N. 1994. Environmental Chemistry, Second Edition. Wuerz Publishing Ltd., Winnipeg, 376 p.

Byers, H. G., Anderson, M. S., Kellogg, C. E., and Thorp, J. 1938. Formation of Soil. 948-978

Canadian Agricultural Services Coordinating Committee. 1998. The Canadian system of soil classification. No. 1646. NRC Research Press.

Canada-US AQA, 2010. Canada-United States Air Quality Agreement: 2010 Progress Report. Environment Canada. ISBN: 978-1-100-17180-7 87. online URL. www.ec.gc.ca/air/default.asp.langEnand;83930AC3-1 92

Cape, J. N. 1993. Direct damage to vegetation caused by acid rain and polluted cloud: definition of critical levels for forest trees. Environmental pollution. 82, 167-180.

Cape, J. N., Fowler, D., and Davison, A. 2003. Ecological effects of sulfur dioxide, fluorides, and minor air pollutants: recent trends and research needs. Environment International. 29, 201-211.

Carter, M. R. 2002. Soil quality for sustainable land management. Agronomy journal. 94, 38-47.

Clague, J.J. 1984. Quaternary Geology and Geomorphology, Smithers–Terrace–Prince Rupert area, British Columbia. Geological Survey of Canada, Memoir No. 413. 71 pp.

Coffey, G. N. 1912. A study of the soils of the United States. Bureau of Soils Bulletin No. 85. US Department of Agriculture, Washington, DC. 23-38.

Cullis, C. F., and Hirschler, M. M. 1980. Atmospheric sulphur: natural and man-made sources. Atmospheric Environment 1967. 14, 1263-1278.

De Kimpe, C. R., Laverdiere, M. R., Dejou, J., and Lasalle, P. 1984. Effects of acidic and basic parent materials on formation of some soils in Quebec (Canada). Geoderma, *33*, 101-118.

Dohrmann, R., Genske, D., Karnland, O., Kaufhold, S., Kiviranta, L., Olsson, S., and Valter, M. 2012. Interlaboratory CEC and exchangeable cation study of bentonite buffer materials: I. Cu II-triethylenetetramine method. Clays and Clay Minerals. 60, 162-175.

Doran, J. W., and Parkin, T. B. 1994. Defining and assessing soil quality. Defining soil quality for a sustainable environment. 1-21.

Dore, A. J., Vieno, M., Tang, Y. S., Dragosits, U., Dosio, A., Weston, K. J., and Sutton, M. A. 2007. Modelling the atmospheric transport and deposition of sulphur and nitrogen over the United Kingdom and assessment of the influence of SO2 emissions from international shipping. Atmospheric environment. 41, 2355-2367.

Dorji, T., Odeh, I., and Field, D. 2014. Vertical distribution of soil organic carbon density in relation to land use/cover, altitude and slope aspect in the eastern Himalayas. Land. 3, 1232-1250.

Driscoll, C. T., Lawrence, G. B., Bulger, A. J., Butler, T. J., Cronan, C. S., Eagar, C., and Weathers, K. C. 2001. Acidic Deposition in the Northeastern United States: Sources and Inputs, Ecosystem Effects, and Management Strategies: The effects of acidic deposition in the northeastern United States include the acidification of soil and water, which stresses terrestrial and aquatic biota. BioScience. 51, 180-198.

Edwards, L., Backhouse, N., Darmstadt, H., and Dion, M. J. (2012). Evolution of anode grade coke quality. Light Metals 2012. 1207-1212.

Egli, M., Fitze, P., and Mirabella, A. (2001). Weathering and evolution of soils formed on granitic, glacial deposits: results from chronosequences of Swiss alpine environments. Catena, 45, 19-47.

Ellis, J. H. 1938. The soils of Manitoba No. 15. Manitoba Economic Survey Board.

Environment Canada. (2018). Canadian Climate Normals: 1981-2010. climate.weather.gc/climate_normals. Accessed 1 September 2018.

ESSA Technologies, J. ESSA, Limnotek, Risk Sciences International, Rio Tinto Alcan, Trent University, Trinity Consultants, and University of Illinois. 2013. Sulphur Dioxide Technical Assessment Report in Support of the 2013 Application to Amend the P2-00001 Multimedia Permit for the Kitimat Modernization Project. Volume 2: Final Technical Report. Prepared for Rio Tinto Alcan, Kitimat, B.C. 450 pp.

Fay, J. A., Golomb, D., and Kumar, S. 1985. Source apportionment of wet sulfate deposition in eastern North America. Atmospheric Environment (1967). 19, 1773-1782.

Fernandez, I. J., Rustad, L. E., Norton, S. A., Kahl, J. S., and Cosby, B. J. 2003. Experimental acidification causes soil base-cation depletion at the Bear Brook Watershed in Maine. Soil Science Society of America Journal, 676, 1909-1919.

Finke, P. A. 2006. Quality assessment of digital soil maps: producers and users' perspectives. Developments in Soil Science, 31, 523-631.

Fox, T. R., and Comerford, N. B. 1990. Low-molecular-weight organic acids in selected forest soils of the southeastern USA. Soil Science Society of America Journal. 54, 1139-1144.

Freedman, B., and Hutchinson, T. C. 1980. Pollutant inputs from the atmosphere and accumulations in soils and vegetation near a nickel–copper smelter at Sudbury, Ontario, Canada. Canadian Journal of Botany. 58, 108-132.

Garland, J. A. 1977. The dry deposition of sulphur dioxide to land and water surfaces. Proceedings of the Royal Society of London. A. Mathematical and Physical Sciences. 354, 245-268.

Gasch, C. K., Hengl, T., Gräler, B., Meyer, H., Magney, T. S., and Brown, D. J. 2015. Spatio-temporal interpolation of soil water, temperature, and electrical conductivity in 3D+ T: The Cook Agronomy Farm data set. Spatial Statistics. 14, 70-90.

Giehl, R. F., and von Wirén, N. 2014. Root nutrient foraging. Plant Physiology. 166, 509-517.

Giesler, R., and Lundström, U. 1993. Soil solution chemistry: effects of bulking soil samples. Soil Science Society of America Journal. 57, 1283-1288.

Grunwald, S., Thompson, J. A., and Boettinger, J. L. 2011. Digital soil mapping and modeling at continental scales: Finding solutions for global issues. Soil Science Society of America Journal. 75, 1201-1213.

Guadalix, M. E., and Pardo, M. T. 1991. Sulphate sorption by variable charge soils. *Journal of soil science*. *42*, 607-614.

Hartemink, A. E., Krasilnikov, P., and Bockheim, J. G. 2010. Soil maps of the world. Geoderma. 207, 256-267.

Hendershot, W. H., Lalande, H., and Duquette, M. 1993. Ion exchange and exchangeable cations. Soil sampling and methods of analysis. 19, 167-176.

Henderson, G. S. 1995. Soil organic matter: A link between forest management and productivity. Carbon forms and functions in forest soils. 419-435.

Hengl, T., Heuvelink, G. B., and Stein, A. 2004. A generic framework for spatial prediction of soil variables based on regression-kriging. Geoderma. 1201, 75-93.

Hengl, T. 2007. A practical guide to geostatistical mappingVol. 52, p. 15.

Hengl, T., de Jesus, J. M., MacMillan, R. A., Batjes, N. H., Heuvelink, G. B., Ribeiro, E., and Gonzalez, M. R. 2014. SoilGrids1km—global soil information based on automated mapping. PloS one. 98.

Hengl, T., de Jesus, J. M., Heuvelink, G. B., Gonzalez, M. R., Kilibarda, M., Blagotić, A., and Guevara, M. A. 2017. SoilGrids250m: Global gridded soil information based on machine learning. PLoS one. 12, e0169748.

Hilgard, E. 1914. Soils. The Macmillian Company. New York.

Hutchinson, T. C., and Whitby, L. M. 1977. The effects of acid rainfall and heavy metal particulates on a boreal forest ecosystem near the Sudbury smelting region of Canada. Water, Air, and Soil Pollution. 74, 421-438.

James, G., Witten, D., Hastie, T., and Tibshirani, R. 2013. An introduction to statistical learning Vol. 112, p. 18. New York: springer.

Jenny, H. 1941. Factors of soil formation: a system of quantitative pedology. New York: McGraw-Hill.

Jobbagy, E. G., and Jackson, R. B. 2001. The distribution of soil nutrients with depth: global patterns and the imprint of plants. Biogeochemistry. 53, 51-77.

Johnson, D. W., Richter, D. D., Miegroet, H. V., and Cole, D. W. 1983. Contributions of acid deposition and natural processes to cation leaching from forest soils: a review. Journal of the Air Pollution Control Association, 33, 1036-1041.

Johnson, C. E. 2002. Cation exchange properties of acid forest soils of the northeastern USA. European Journal of Soil Science. 532, 271-282.

Johnson, C. E., Driscoll, C. T., Siccama, T. G., and Likens, G. E. 2000. Element fluxes and landscape position in a northern hardwood forest watershed ecosystem. Ecosystems. 32, 159-184.

Johnson, C. E., Ruiz-Méndez, J. J., and Lawrence, G. B. 2000. Forest soil chemistry and terrain attributes in a Catskills watershed. Soil Science Society of America Journal. 64, 1804-1814.

Jones, D. L. 1998. Organic acids in the rhizosphere–a critical review. Plant and soil. 205, 25-44.

Joslin, J. D., Kelly, J. M., and Van Miegroet, H. 1992. Soil chemistry and nutrition of North American spruce-fir stands: evidence for recent change. Journal of Environmental Quality. 21, 12-30.

Khoder, M. I. 2002. Atmospheric conversion of sulfur dioxide to particulate sulfate and nitrogen dioxide to particulate nitrate and gaseous nitric acid in an urban area. Chemosphere. 49, 675-684.

Kline, J. R. 1973. Mathematical Simulation of Soil-Plant Relationships and Soil GENESIS1. Soil Science. 115, 240-249

Kochian, L. V., Pineros, M. A., and Hoekenga, O. A. 2005. The physiology, genetics and molecular biology of plant aluminum resistance and toxicity. In Root physiology: from gene to function pp. 175-195. Springer, Dordrecht.

Kellogg, W. W., Cadle, R. D., Allen, E. R., Lazrus, A. L., and Martell, E. A. 1972. The sulfur cycle. Science. 17540, 587-596.

Krajina, V. J. 1975. Some observations on the three subalpine biogeoclimatic zones in British Columbia, Yukon and Mackenzie District. Phytocoenologia. 396-400.

Larson, W. E., and Pierce, F. J. 1991. Conservation and enhancement of soil quality. In Evaluation for sustainable land management in the developing world. IBSRAM Proceedings Thailand. 15-21 September 1991.

Lawrence, G. B., Fernandez, I. J., Richter, D. D., Ross, D. S., Hazlett, P. W., Bailey, S. W., and Kaste, J. M. 2013. Measuring environmental change in forest ecosystems by repeated soil sampling: a North American perspective. Journal of Environmental Quality. 423, 623-639.

Leiningen, W. Z. 1909. Über Humusablagerungen im Gebiete der Zentralalpen. Naturw. Z. Forst-Landw. 6, 10.

Levasseur, P. "Estimating Mineral Surface Area and Acid Sensitivity of Forest Soils in Kitimat, British Columbia." MS, Trent University, 2018.

Likens, G. E., Bormann, F. H., Johnson, N. M., and Pierce, R. S. 1967. The calcium, magnesium, potassium, and sodium budgets for a small forested ecosystem. Ecology, 48(5), 772-785.

Likens, G. E., Driscoll, C. T., Buso, D. C., Siccama, T. G., Johnson, C. E., Lovett, G. M. and Reiners, W. A. 1994. The biogeochemistry of potassium at Hubbard Brook. Biogeochemistry, 25, 61-125.

Likens, G. E., Driscoll, C. T., Buso, D. C., Siccama, T. G., Johnson, C. E., Lovett, G. M., and Bailey, S. W. 1998. The biogeochemistry of calcium at Hubbard Brook. Biogeochemistry. 41, 89-173.

Marbut, C. F. 1935. Soils of the United States, Atlas of American Agriculture, Part III. US Department of Agriculture, Washington, DC.

McBratney, A. B., Odeh, I. O., Bishop, T. F., Dunbar, M. S., and Shatar, T. M. 2000. An overview of pedometric techniques for use in soil survey. Geoderma. 973, 293-327.

Meidinger, D., & Pojar, J. 1991. Ecosystems of British Columbia. *Special Report Series-Ministry of Forests, British Columbia*. 6.

Moore, I. D., Turner, A. K., Wilson, J. P., Jenson, S. K., and Band, L. E. 1993. GIS and land-surface-subsurface process modeling. Environmental modeling with GIS. 20, 196-230.

Mongeon, A., Aherne, J., and Watmough, S. A. 2010. Steady-state critical loads of acidity for forest soils in the Georgia Basin, British Columbia. Journal of Limnology, 193-200.

Mylona, S. 1996. Sulphur dioxide emissions in Europe 1880–1991 and their effect on sulphur concentrations and depositions. Tellus B. 48, 662-689.

Nilsson, J. 1988. Critical loads for sulphur and nitrogen. In Air pollution and Ecosystems. pp. 85-91. Springer, Dordrecht.

Nilsson, J., and Grennfelt, P. 1988. Critical Loads for Sulphur and Nitrogen. Miljörapport 1988: 15. In Workshop at Skokloster, Sweden. pp. 19-24.

Nuotio, T., Hyyppä, J., and Nylander, E. 1990. Buffering capacity of Finnish soils and its dependence on geological factors in relation to the acidification sensitivity of lakes. In Acidification in Finland pp. 271-286. Springer, Berlin, Heidelberg.

Oh, N. H., and Richter Jr, D. D. 2004. Soil acidification induced by elevated atmospheric CO2. Global Change Biology. 10, 1936-1946.

Omuto, C., Nachtergaele, F., and Vargas Rojas, R. 2012. State of the Art Report on Global and Regional Soil Information: Where are we? Where to go? FAO, Italy. 69 p.

Osher, L. J., and Buol, S. W. 1998. Relationship of soil properties to parent material and landscape position in eastern Madre de Dios, Peru. Geoderma. 83, 143-166.

Ouimet, R., and Duchesne, L. 2005. Base cation mineral weathering and total release rates from soils in three calibrated forest watersheds on the Canadian Boreal Shield. Canadian Journal of Soil Science. 85, 245-260.

Ouimet, R., Arp, P. A., Watmough, S. A., Aherne, J., and DeMerchant, I. 2006. Determination and mapping critical loads of acidity and exceedances for upland forest soils in Eastern Canada. Water, Air, and Soil Pollution. 172, 57-66.

Pebesma, E. J. 2004. Multivariable geostatistics in S: the gstat package. Computers and Geosciences. 30, 683-691.

Piirainen, S., Finér, L., and Starr, M. 2002. Deposition and leaching of sulphate and base cations in a mixed boreal forest in eastern Finland. Water, Air, and Soil Pollution. 133, 185-204.

Phillips, J. D. 1998. On the relations between complex systems and the factorial model of soil formation with discussion. Geoderma. 86, 1-21.

Phillips, J. D., Turkington, A. V., and Marion, D. A. 2008. Weathering and vegetation effects in early stages of soil formation. Catena. 72, 21-28.

QGIS Development Team 2016. QGIS Geographic Information System. Open Source Geospatial Foundation Project. http://qgis.osgeo.org

Reganold, J. P., and Palmer, A. S. 1995. Significance of gravimetric versus volumetric measurements of soil quality under biodynamic, conventional, and continuous grass management. Journal of Soil and Water Conservation. 50, 298-305.

Reuss, J. O., and Johnson, D. W. 1986. Acid deposition and the acidification of soils and waters Vol. 59. Springer Science and Business Media.

Ruess, L., Sandbach, P., Cudlín, P., Dighton, J., and Crossley, A. 1996. Acid deposition in a spruce forest soil: effects on nematodes, mycorrhizas and fungal biomass. Pedobiologia. 40, 51-66.

Reuss, J. O., Cosby, B. J., and Wright, R. F. 1987. Chemical processes governing soil and water acidification. Nature. 6134, 27.

Richardson, J. L., and Edmonds, W. J. 1987. Linear regression estimations of Jenny's relative effectiveness of state factors equation. Soil science. 144, 203-208.

Romig, D. E., Garlynd, M. J., and Harris, R. F. 1996. Farmer-Based Assessment of Soil Quality: A Soil Health Scorecard 1. Methods for assessing soil quality. 39-60.

Rosenstock, N. P., Stendahl, J., van der Heijden, G., Lundin, L., McGivney, E., Bishop, K., and Löfgren, S. 2019. Base cations in the soil bank. Non-exchangeable pools may sustain centuries of net loss to forestry and leaching. Unpublished. https://www. soil-discuss. net/soil-2019-5/,2019-04-25.

Schlesinger, W. H. 1977. Carbon balance in terrestrial detritus. Annual review of ecology and systematics. 8, 51-81.

Schut, P., Smith, S., Fraser, W., Geng, X., and Kroetsch, D. 2011. Soil landscapes of Canada: building a national framework for environmental information. Geomatica. 65, 293-309.

Schoenholtz, S. H., Van Miegroet, H., and Burger, J. A. 2000. A review of chemical and physical properties as indicators of forest soil quality: challenges and opportunities. Forest ecology and management. 138, 335-356.

Schwartz, S. E. 1989. Acid deposition: unraveling a regional phenomenon. Science. 243, 753-763.

Sims, T. J. 1996. Lime requirement. *In*: D. L. Sparks (Editor), Methods of Soil Analysis. Part 3 Chemical Methods. Soil Sci. Soc. of Am. Book Series no. 5. Agronomy, 17:491-515.

Sonon, L. S., Kissel, D. E., and Saha, U. 2014. Cation exchange capacity and base saturation. UGA Extension Circular. 1040, 1-4.

Spranger, T., Hettelingh, J. P., Slootweg, J., and Posch, M. 2008. Modelling and mapping long-term risks due to reactive nitrogen effects: an overview of LRTAP convention activities. Environmental Pollution. 154, 482-487.

Statistics Canada. 2016. 2016 Census profile: British Columbia. Retrieved September 27, 2017 from Statistics Canada: https://www12.statcan.gc.ca/census-recensement/2016/dp-

pd/prof/details/page.cfm?Lang=EandGeo1=POPCandCode1=0420andGeo2=PRandCode2=59andSearchText=KitimatandSearchType=BeginsandSearchPR=01andB1=AllandGeoLevel=PRandGeoCode=0420andTABID=1andtype=0

Stantec (Stantec Consulting Ltd.) 2014. Emissions Assessment for Soils and Vegetation Technical Assessment Report Prepared by Stantec Consulting Ltd. for LNG Canada Development Inc. (LNG Canada).

Stephens, C. G. 1947. Functional synthesis in pedogenesis. Philosophical Transactions of the Royal Society. Aust, 7. 168-181.

Sumner, M. E., and Miller, W. P. 1996. Cation exchange capacity and exchange coefficients. Methods of soil analysis part 3—chemical methods. 1201-1229.

Tamminen, P., and Starr, M. R. 1990. A survey of forest soil properties related to soil acidification in southern Finland. In Acidification in Finland pp. 235-251. Springer, Berlin, Heidelberg.

Thomas, G. W. 1982. Exchangeable cations. *In*: A. L. Page (Editor), Methods of Soil Analysis. Part 2. 2nd ed. Agronomy, 9:159-165.

Tucker, B. M. 1985. Active and exchangeable cations in soils. *Soil Research. 23,* 195-209.

Turner, B. F., Stallard, R. F., and Brantley, S. L. 2003. Investigation of in situ weathering of quartz diorite bedrock in the Rio Icacos basin, Luquillo Experimental Forest, Puerto Rico. Chemical Geology, 202, 313-341.

UBA 2004. Manual on methodologies and criteria for modelling and mapping of critical loads and levels and air pollution effects, risks and trends. Umweltbundesamt, Dessau, Germany. Retrieved from http://www. icpmapping.org

United Nations. Economic Commission for Europe. 2004. Handbook for the 1979 Convention on Long-range Transboundary Air Pollution and Its Protocols. United Nations Publications.

van Breemen, N., Driscoll, C. T., and Mulder, J. 1984. Acidic deposition and internal proton sources in acidification of soils and waters. Nature. 307, 599.

van't Hoff, J. H. 1884. Etudes de dynamique chimique, Amsterdam, F. Miller and Co.

von Lützow, M., and Kögel-Knabner, I. 2009. Temperature sensitivity of soil organic matter decomposition—what do we know? Biology and Fertility of soils, 46, 1-15.

Waksman, S. A., and Gerretsen, F. C. 1931. Influence of temperature and moisture upon the nature and extent of decomposition of plant residues by microorganisms. Ecology. 12, 33-60.

Whitfield, C. J., and Reid, C. 2013. Predicting surface area of coarse-textured soils: Implications for weathering rates. Canadian Journal of Soil Science. 93, 621-630.

Williston, P., Aherne, J., Watmough, S., Marmorek, D., Hall, A., de la Cueva Bueno, P., and Laurence, J. A. 2016. Critical levels and loads and the regulation of industrial emissions in northwest British Columbia, Canada. Atmospheric environment. 146, 311-323.

Wu, J., Zhang, R., and Gui, S. 1999. Modeling soil water movement with water uptake by roots. Plant and soil. 215, 7-17.

6.0 APPENDIX

Table A1. Site characteristics (sample ID, latitude, longitude, slope (degrees, total precipitation [mm], annual minimum, maximum, and mean temperature [°C], vegetation cover [%] and elevation [m] for all 72 locations sampled in the Kitimat Valley, British Columbia

Sample ID	Latitude	Longitude	Slope (degrees)	Total Precipitation (mm)	Annual Max Temp (°C)	Annual Min temp (°C)	Annual Mean temp (°C)	Vegetation Cover (%)	Elevation (m)
A01	54.21106	-128.73848	11	2016	9	1	5	39.8	1114
A02	54.27010	-128.72496	4	1564	6	-1	3	39.8	1287
A03	54.29795	-128.70241	19	1864	8	1	5	40.7	1132
A04	54.31601	-128.69710	5	1682	8	0	4	90.5	1150
A05	54.21925	-128.74606	21	2016	9	1	5	52.5	823
CA004	54.04152	-128.68081	0	2982	11	3	7	96.0	22
CA008	54.42818	-128.64065	2	1916	11	3	7	100.0	115
DCAS08-01	54.63180	-128.38968	11	1218	8	0	4	100.0	428
DCAS08-03	54.65358	-128.67977	12	1470	9	1	5	100.0	251
DCAS08-04	54.66512	-128.61191	20	1194	5	-2	2	95.8	706
DCAS21	54.01498	-128.77339	9	2485	9	2	5	91.2	383
DCAS23	53.93945	-128.61989	15	2530	9	2	6	90.8	317
DCAS25	54.44968	-128.56120	1	1783	10	3	7	97.7	213
DCAS26	54.29403	-128.60201	1	2111	11	3	7	97.7	208
DCAS27	54.03402	-128.64607	0	3012	11	3	7	96.8	14
DCAS28	54.05195	-128.70460	5	2982	11	3	7	96.8	166
DCAS29	54.12220	-128.67442	2	2679	11	3	7	96.8	66
E01	54.01448	-128.71008	21	3088	11	3	7	94.7	94
E02	54.02568	-128.71893	12	2832	10	3	6	96.8	126
G0026	54.25446	-128.74971	19	1564	6	-1	3	100.0	365
G0027	54.25651	-128.74990	25	1564	6	-1	3	100.0	454
G0028	54.24928	-128.75694	5	1903	8	1	4	74.5	193

GD003	54.33821	-128.53953	6	2020	11	3	7	99.8	163
GD009	54.32926	-128.50122	11	1511	8	0	4	100.0	342
GD012	54.23872	-128.45539	2	1988	10	2	6	99.8	150
GD013	54.47267	-128.50635	5	1703	11	3	7	96.8	206
G0008	54.24385	-128.73980	5	2016	9	1	5	100.0	183
GR001	54.33452	-128.86574	23	1586	6	-1	3	100.0	580
GR002	54.43693	-128.68596	4	1949	11	3	7	99.8	106
GR003	54.44129	-128.67800	7	1949	11	3	7	100.0	142
GR005	54.34788	-128.86517	36	2069	9	2	5	69.7	543
JD132	54.283	-128.592	0	2175	11	3	7	97.5	204
JD312	54.24	-128.643	3	2342	11	3	7	99.8	243
L01	54.31455	-128.64862	4	2089	10	2	6	99.8	231
L02	54.33215	-128.63716	6	2059	11	3	7	100.0	168
L03	54.33066	-128.62736	4	2059	11	3	7	99.8	152
L28	54.08047	-128.70444	6	2982	11	3	7	96.5	94
LM001	54.52327	-128.42997	26	1396	9	1	5	94.2	379
LM006	54.46008	-128.64799	9	1821	11	3	7	100.0	103
LM009	54.46428	-128.65605	5	1821	11	3	7	100.0	139
LM010	54.46430	-128.65887	5	1821	11	3	7	100.0	139
OG001	54.31242	-128.86160	12	1586	6	-1	3	78.7	660
OG003	54.37558	-128.86519	30	2176	10	3	7	70.7	396
OG009	54.31740	-128.86314	11	1586	6	-1	3	77.2	624
OG010	54.31849	-128.86413	7	1586	6	-1	3	75.7	609
P01	54.47381	-128.56547	3	1728	11	3	7	99.8	229
QD007	54.28023	-128.62490	0	2210	10	3	7	100.0	199
QD012	54.37517	-128.58013	4	1918	11	3	7	99.8	86
QD015	54.04485	-128.59393	10	2408	10	2	6	100.0	135
QM001	53.98738	-128.64631	17	3007	11	3	7	98.8	119
QM002	54.00672	-128.63648	23	3012	11	3	7	91.8	144
QM003	53.98342	-128.64679	21	3007	11	3	7	96.5	129

QM005	53.99821	-128.64567	15	3012	11	3	7	98.7	117
S01	53.09146	-128.79173	6	2745	9	2	6	90.2	108
S006	54.58062	-128.70652	5	1642	11	3	7	99.8	217
S011	54.59437	-128.68563	6	1642	11	3	7	97.7	210
S02	53.94606	-128.73470	8	3349	11	3	7	100.0	138
S022	54.59005	-128.68474	1	1642	11	3	7	97.7	216
S03	53.93431	128.72674	9	3349	11	3	7	85.8	99
SSS001	53.96930	-128.63697	9	3007	11	3	7	99.7	117
SSS003	54.10934	-128.73578	10	2281	9	2	5	96.5	394
SSS006	54.58559	-128.67827	3	1642	11	3	7	99.8	220
SS1	54.02652	-128.70317	1	3088	11	3	7	89.2	10
SSS005	54.40207	-128.84686	3	2176	10	3	7	97.0	57
VA001	54.52647	-128.71312	11	1731	10	2	6	99.8	98
VA002	54.54578	-128.71266	20	1657	10	2	6	99.5	263
VA006	54.52128	-128.71516	5	1731	10	2	6	99.8	77
VA012	54.55849	-128.71606	6	1657	10	2	6	97.7	174
VC001	54.45235	-128.65294	3	1949	11	3	7	100.0	101
VC002	54.44569	-128.82513	12	2119	11	3	7	99.8	61
VC003	54.44677	-128.64617	1	1916	11	3	7	99.8	114
VC005	54.45058	-128.63932	2	1838	11	3	7	99.8	119

Table A2. Parameter, file name, and variable description of all 91 continuous maps used to complete regression kriging in the Kitimat Valley, British Columbia.

Parameter	File names	Variable description
Climate variables	sg_01	julian day number of start of the growing season
	sg_02	julian day number at end of the growing season
	sg_03	number of days of the growing season
	sg_04	total precipitation for period 1
	sg_05	total precipitation for period 2
	sg_06	total precipitation for period 3
	sg_07	total precipitation for period 4
	sg_08	gdd above base_temp for period 1
	sg_09	gdd above base_temp for period 2
	sg_10	gdd above base_temp for period 3
	sg_11	gdd above base_temp for period 4
	sg_12	annual mean temperature
	sg_13	annual minimum temperature
	sg_14	annual maximum temperature
	sg_15	mean temperature for period 3
	sg_16	temperature range for period 3
Soil variables	BDTICM_M_250m	absolute depth to bedrock
	BLDFIE_M_sl3_250m	bulk density @ 15cm
	BLDFIE_M_sl4_250m	bulk density @ 30cm
	CECSOL_M_sl3_250m	CEC @ 15cm
	CECSOL_M_sl4_250m	CEC @ 30cm
	CLYPPT_M_sl3_250m	Clay % @ 15cm
	CLYPPT_M_sl4_250m	Clay % @ 30cm
	CRFVOL_M_sl3_250m	Coarse fragment volume @ 15cm
	CRFVOL_M_sl4_250m	Coarse fragment volume @ 30cm
	ORCDRC_M_sl3_250m	Organic carbon @ 15cm
	ORCDRC_M_sl4_250m	Organic carbon @ 30cm
	PHIHOX_M_sl3_250m	pH H2O @ 15cm
	PHIHOX_M_sl4_250m	pH H2O @ 30cm

	SNDPPT_M_sl3_250m	Sand % @ 15 cm
	SNDPPT_M_sl4_250m	Sand % @ 30 cm
Runoff	Q	Runoff
DEM	DEM	Digital elevation model
	SLOPE	Slope in degrees (from DEM)
Geology variables	andesite	
	andesite, basalt, volcanic sandstone, rhyolite	
	andesite breccia, lapilli tuff	
	andesite, dacite, volcaniclastics	
	andesitic volcanic rocks	
	argillite, chert, limy shale	
	argillite, siltstone, chert	
	calc-silicate, limestone, marble	
	conglomerate, breccia	
	conglomerate, carbonate	
	conglomerate, sandstone, siltstone	
	dacite, rhyolite	
	diorite	
	diorite, gabbro	
	diorite, gabbro, quartz diorite, granodiorite	
	diorite, granodiorite, tonalite, gabbro	
	diorite, granodiorite, tonalite, metagabbro	
	diorite, microdiorite, gabbro	
	gabbroic, diorite	
	gabbro, pyroxenite, diorite	
	granite	
	granite, granodiorite	
	granite, granodiorite, diorite	
	granodiorite	
	granodiorite, granite	
	granodiorite, tonalite, granite	

granodioritic intrusive rocks
granodioritic orthogneiss
intrusive rocks, undivided
limestone, cherty limestone
limestone, marble, calcareous sedimentary rocks
limestone, marble, silty limestone, mudstone, lapilli tuff
marble, calc-silicate
meta-andesite, metabasalt, metarhyolite
meta-andesite, metabasalt, metarhyolite - altered
metabasalt
mylonitic orthogneiss
orthogneiss
orthogneiss metamorphic rocks
quartz diorite
quartz dioritic intrusive rocks
quartz-sericite schist
rhyolite
rhyolite, basalt
rhyolite dike
rhyolite dikes
sandstone, siltstone, argillite, conglomerate, basalt
sandstone, siltstone, shale, coal
sedimentary rocks, undivided
tonalite, diorite
tonalite, quartz diorite
tuff
undivided intrusive rocks
volcanic rocks, undivided
volcanic sandstone, siltstone

	volcanic sandstone, siltstone, tuff
Forest variables	LandCover_NonVeg
	LandCover_VegNonTreed
	LandCover_VegTreed
	LandCover_Veg
	Species_Abie_Ama
	Species_Abie_Bal
	Species_Abie_Las
	Species_Abie_Spp
	Species_Pice_Eng_Gla
	Species_Pice_Eng
	Species_Pice_Mar
	Species_Pice_Rub
	Species_Pice_Sit
	Species_Pice_Spp
	Species_Pinu_Con
	Species_Pinu_Mon
	Species_Pinu_Pon
	Species_Pinu_Str
	Species_Popu_Tre
	Species_Pseu_Men_Men
	Species_Pseu_Men
	Species_Thuj_Pli
	Species_Tsug_Can
	Species_Tsug_Het
	Species_Tsug_Mer
	Species_Tsug_Spp
	Structure_Biomass_Branch
	Structure_Biomass_Foliage
	Structure_Biomass_StemBark
	Structure_Biomass_StemWood
	Structure_Biomass_TotalDead

Structure_Biomass_TotalLiveAboveGroun
d
Structure_Stand_Age
Structure_Stand_CrownClosure
Structure_Stand_Height
Structure_Volume_Merch
Structure_Volume_Total

Table A1. Average, coefficient of variation (CV; %), minimum and maximum for all soil properties (bulk density, coarse fragment, organic matter, sand, silt and clay, exchangeable [Ex] acidity and Ex cations) at all sampling depths (0-10 cm, 15-25 cm, and 40-50 cm) for all 72 sampling locations in the Kitimat Valley, British Columbia.

Parameter	Units	Average			CV%			Minimum			Maximum		
Soil depth	cm	0-10	15-25	40-50	0-10	15-25	40-50	0-10	15-25	40-50	0-10	15-25	40-50
Bulk density	g/cm3	0.59	0.75	0.83	48.58	37.05	46.48	0.09	0.09	0.13	1.19	1.39	2.00
Coarse fragment	%	14.89	18.51	21.43	120.47	101.24	88.4	0.00	0.00	0.00	80.61	93.68	65.91
Organic matter	%	17.53	12.62	8.85	94.18	81.86	97.10	2.60	1.94	1.81	89.48	52.78	61.67
Sand	%	50.45	52.68	53.11	38.88	36.38	33.99	13.08	15.86	13.51	99.31	98.47	97.90
Silt	%	44.26	42.55	42.46	41.30	39.76	38.22	0.69	1.29	1.97	77.68	72.13	75.84
Clay	%	4.93	4.51	4.04	105.24	76.20	74.09	0.00	0.12	0.14	37.40	16.39	13.73
pH (H_2O)		4.6	5.0	5.3	162.25	142.50	92.78	3.7	4.0	4.7	6.5	6.6	6.6
Ex acidity	meq/100g	3.95	2.77	2.04	64.32	65.36	81.06	0.13	0.53	0.13	15.13	8.53	8.60
Ex calcium	meq/100g	1.92	1.43	1.78	128.01	153.09	138.92	0.05	0.04	0.02	14.53	13.23	11.30
Ex potassium	meq/100g	0.16	0.11	0.10	78.96	70.35	82.98	0.02	0.02	0.02	0.83	0.41	0.45
Ex magnesium	meq/100g	0.5	0.31	0.43	114.62	127.75	175.93	0.04	0.03	0.01	3.66	2.53	4.20
Ex sodium	meq/100g	0.08	0.06	0.10	218.24	184.89	300.96	0.00	0.00	0.01	1.35	0.84	2.42
Ex aluminum	meq/100g	0.47	0.48	0.38	121.84	89.50	79.19	0.00	0.00	0.00	4.33	2.39	1.39
Ex iron	meq/100g	0.05	0.04	0.03	98.65	95.92	86.64	0.00	0.00	0.00	0.32	0.25	0.13
Ex manganese	meq/100g	0.05	0.02	0.01	207.49	178.82	136.98	0.00	0.00	0.00	0.58	0.18	0.11

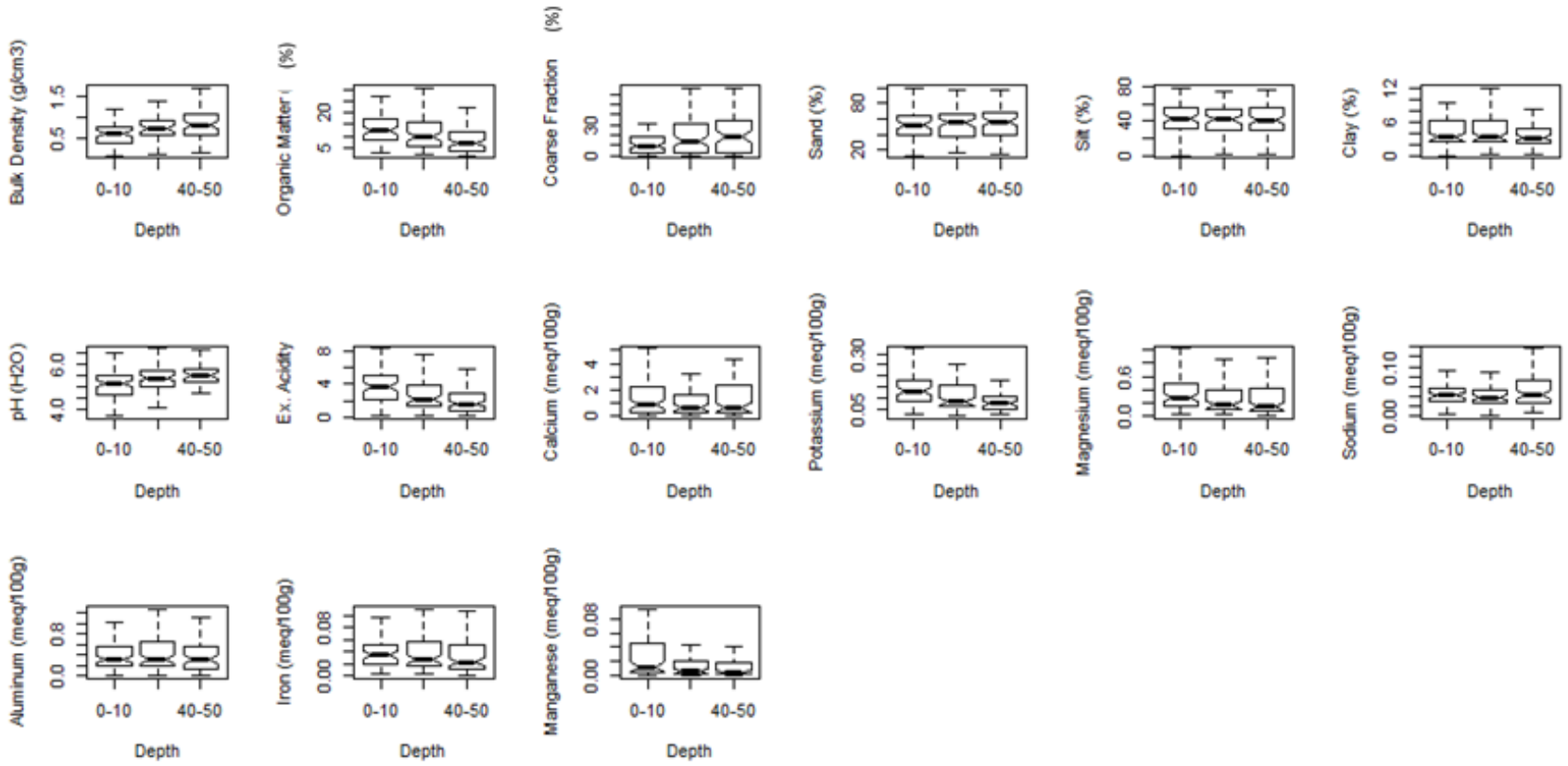

Figure A1. Boxplot comparison of all soil properties (bulk density, coarse fragment, organic matter, sand, silt and clay, exchangeable [Ex] acidity and Ex cations) at the 0-10 cm, 15-25 cm, and 40-50cm depths.

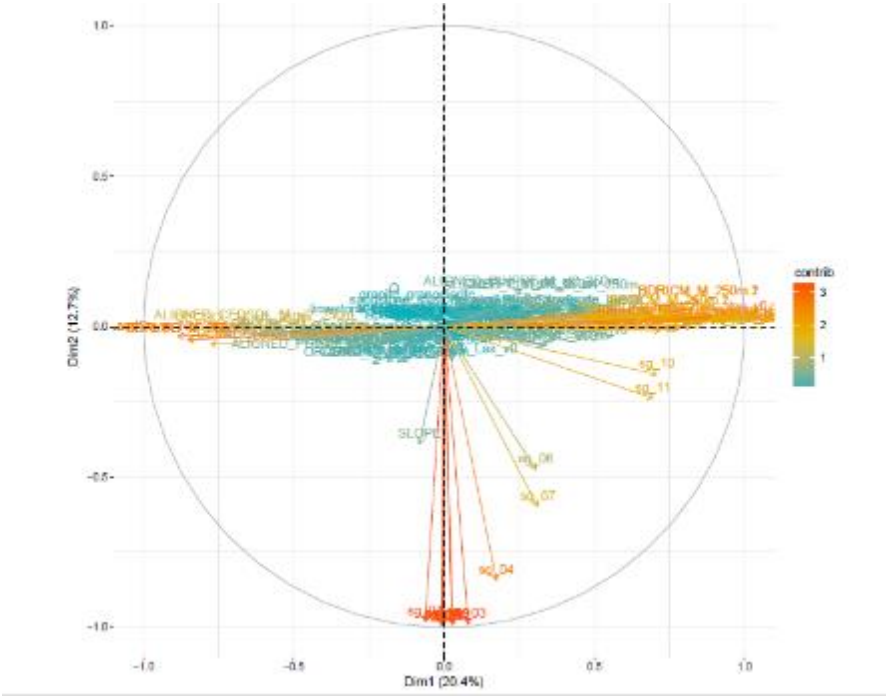

Figure A2. A contribution map indicating the loading of all 91 predictor variables to the first and second SPC's.

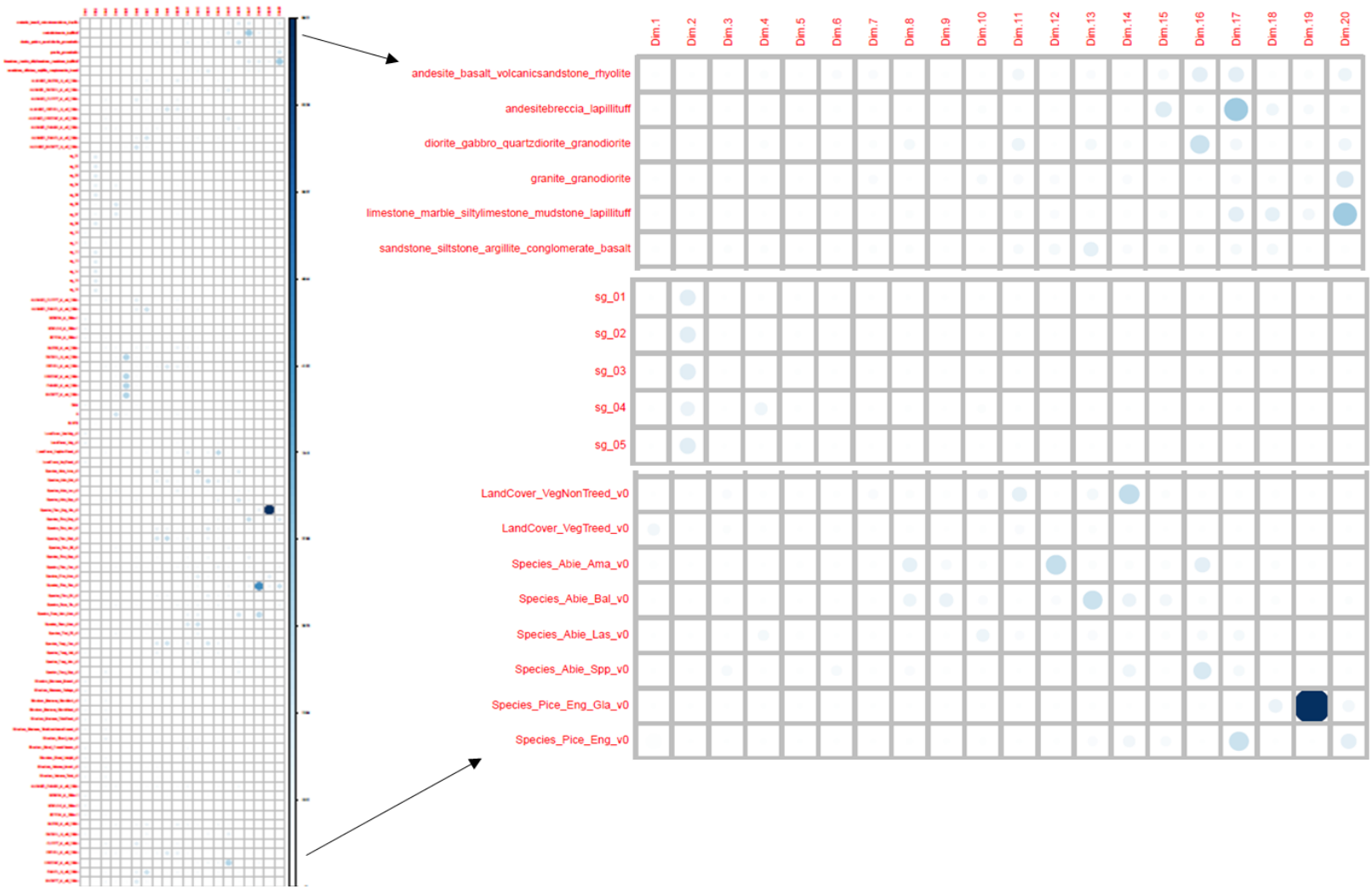

Figure A3. An SPC 'heatmap' and magnified examples, indicating the strongest predictor variables for the SPC's 1-20.

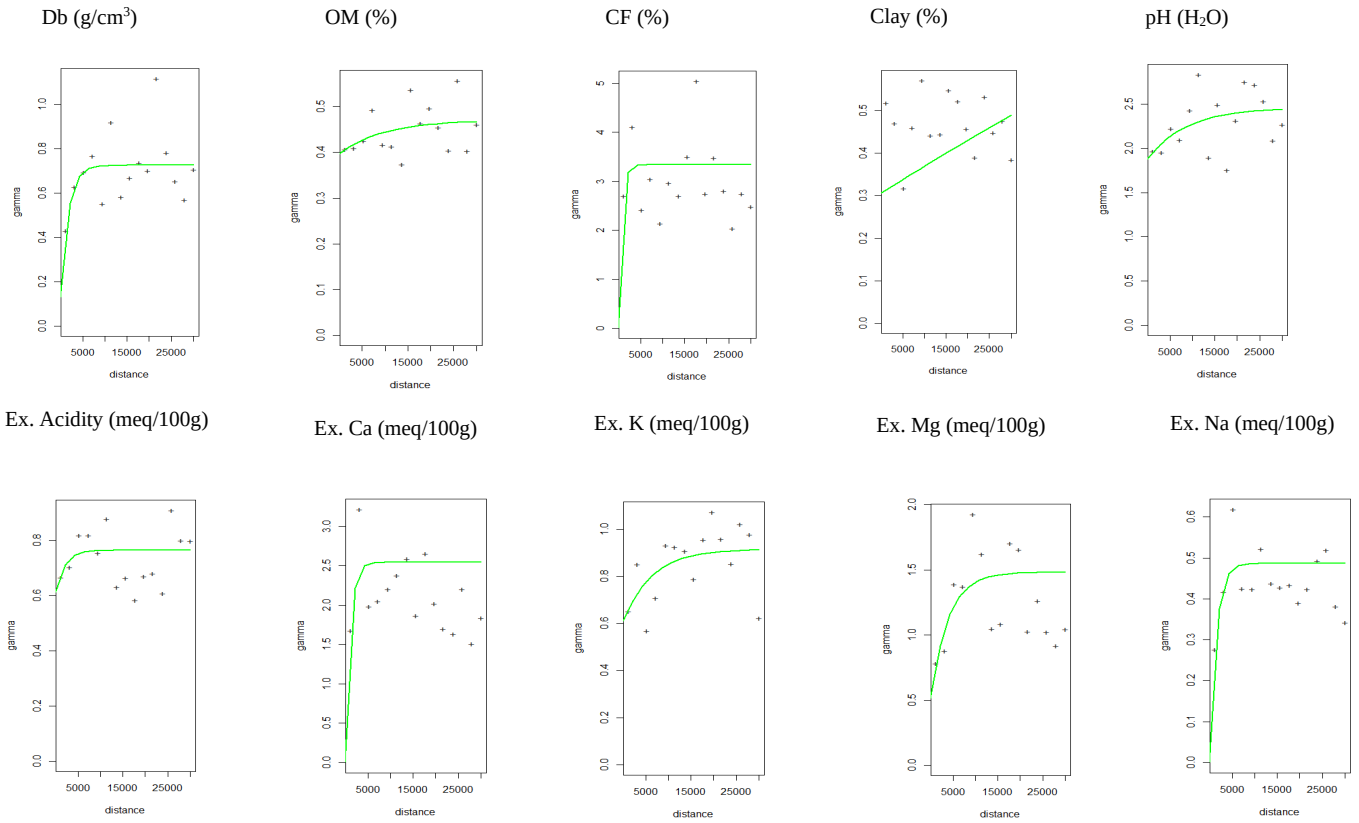

Figure A4. Semivariograms fitted to the residuals of soil properties (bulk density [Db], coarse fragment [CF], organic matter, sand, silt and clay, exchangeable [Ex] acidity and Ex cations) at the weighted average soil depth of 0-50 cm.